LA-UR-08-2694

Approved for public release;
distribution is unlimited.

Title: ANALYTIC VERIFICATION OF MCNP'S NEW PULSE-HEIGHT TALLY WITH VARIANCE REDUCTION FEATURE

Author(s): AVNEET SOOD -- LANL, X-3 MCC
R. ARTHUR FORSTER - LANL, X-3 MCC

Intended for: INTERNAL DOCUMENTATION
APRIL 2008

Form 836 (7/06)

Analytic Verification of MCNP's New Variance Reduction with Pulse-Height Tallies

Los Alamos National Laboratory Report: LA-UR-08-2694

Avneet Sood and R. Arthur Forster
Los Alamos National Laboratory,
Applied Physics (X) Division,
X-3 Computational Simulation and Analysis Group,
P.O. Box 1663, MS A143,
Los Alamos, NM 87545

May 22, 2008

Abstract

One method of code verification includes comparison of calculated results with analytic solutions. For radiation transport, exact solutions to the particle transport equations in three-dimensional space as a function of energy, angle, and time are complex and often impossible. One technique to provide analytic solutions is to simplify or eliminate terms in the transport equation (e.g. one dimension, single energy group, isotropic scattering, ...). An alternative approach to generating analytic solutions is to simplify the nuclear or atomic data, leaving the mathematical equations and computer code unaltered. This probabilistic approach allows analytic solutions to both Boltzmann and non-Boltzmann problems. In this work, we improve on an existing probabilistic approach to analytically verify the non-Boltzmann pulse-height tally in the Monte Carlo code MCNP. This verification is particularly important with the upcoming release of MCNP 5.1.50 which, for the first time, allows almost all of MCNP's variance reduction techniques to be used with pulse-height tallies. The analytic photon-like pulse-height problem is defined for a two-region detector. MCNP calculations of the pulse-height tallies using almost all of the variance reduction methods individually were performed and analyzed. A few extremely subtle bugs were discovered with this verification process. The newly released version of MCNP 5.1.50 with variance reduction for pulse-height tallies has been successfully verified with this problem for many variance reduction techniques available in MCNP 5.1.50.

Introduction

MCNP[1] is a Monte Carlo code used worldwide to model radiation transport in many different applications. Verification and validation of new coding is required to satisfy MCNP software quality assurance requirements and to give users more confidence in the calculated results. One approach for the verification process is to compare calculated results with a problem that has a known analytic solution. One difficulty with analytic verification is that even the simplest transport problems are subject to complex physical laws and are difficult to solve analytically. The physics, data, and/or geometry must be simplified to obtain analytic solutions.

The MCNP pulse-height tally is defined to be the difference in the particle energy entering a cell and the energy leaving that cell for an entire particle history. The energy deposited includes all progeny of the initial source particle. The amount of energy deposited in a cell is the energy pulse for that history. The pulse-height tally in MCNP is analogous to the voltage pulse-height seen in a radiation detector. This tally is unique among the various tallies in MCNP: the entire history must be completed before the pulse-height tally can be made.

Applying variance reduction for pulse-height tallies requires additional detailed bookkeeping for the components of the particle history. The theoretical basis for applying variance reduction to this class of problems has been given in [2, 3]. The bookkeeping requirements are much more complicated than standard variance reduction techniques that apply to Boltzmann-type flux tallies typical in a Monte Carlo calculation because the variance reduction technique can be applied as soon as the particle exits or collides in a cell. Detailed storage of the variance reduction information for the complete history track is not required for Boltzmann-type flux tallies. Variance reduction with pulse-height tallies for photons and electrons is a feature implemented in the next release of MCNP (version 5.1.50) [4]. Tallies that depend on the collective effects of groups of particles (e.g. joint particle density functions) for a history cannot be obtained from the standard Boltzmann transport equation [2] making analytic verification with the usual simplifications not applicable.

The purpose of this research note is to:

1. provide a completely described two detector pulse-height problem with an analytic solution;

2. provide high-precision numerical results from the analytic problem for surface currents, surface fluxes, volume fluxes, energy deposited, and pulse-height spectra;

3. provide verification of MCNP's newly implemented variance reduction for pulse-height tallies using the analytic problem.

Shuttleworth[5] has cleverly devised a set of fictitious nuclides with simplified physical interactions to define several types of verification problems with analytic solutions. His analytic approach for the pulse-height tally uses three fictitious nuclides with a simple geometry. The problem is continuous in space and discrete in energy and angle. The cross sections are constant with energy, angle, and time, and allow for threshold reactions with particle progeny and multiplying reactions. Shuttleworth did not completely solve the analytic problem and reported only a few analytic results [6]. We have completely solved his analytic test problem by finding for all possible collisional probabilities and generating high-precision analytic

results for particle currents, surface and volume fluxes, and pulse-heights for each of the detector regions. We compare our analytic results with analog MCNP calculations using photon and coupled photon-electron transport. Furthermore, we compare the calculations using most of the variance reduction techniques for photons available in MCNP.

The Problem

The pulse-height verification problem originally defined by Shuttleworth consists of a two region cylindrical detector made of three different fictitious nuclides. Shuttleworth defines the nuclide's photon-like reactions and the detector material atom fractions as:

- Moron, atom fraction 0.2
  At all energies, a moron collision absorbs the incident particle.

- Odium, atom fraction 0.3
  At all energies, an odium collision produces one secondary particle that has half the energy of the incident particle. The secondary particle is not deflected.

- Kneeon, atom fraction 0.5
  At all energies, a kneeon collision produces two secondary particles, each having $1/4^{th}$ of the energy of the incident particle. At, or above an incident energy of 1.0 MeV, one particle is scattered forwards and one particle is scattered through 90° . Below 1.0 MeV, both particles are scattered forwards.

These three nuclides represent the photon physical interactions of photoelectric absorption (moron), Compton scatter (odium), and pair production (kneeon). The collision physics of these nuclides are summarized pictorially in figure 1. Each nuclide's individual total microscopic cross section, σ_t, is conveniently set to:

$$\sigma_t = \frac{\text{Material tomic weight}}{\text{Avogadro}'\text{s number x } 10^{-24} \text{ x } \rho}$$

where ρ is the detector gram density. This definition of σ_t makes each nuclide's individual total macroscopic cross section equal to one in units of cm^{-1}. The total macroscopic cross section, Σ_t, of any mixture of these nuclides is therefore also 1.0 cm^{-1}.

The problem geometry is a cylindrical detector divided into two equal volumes, as shown in figure 2. Each detector region is a cylinder of length ln(2) and radius ln(2). A source is located at the center (r=0) of the cylinder axis at L=0 and is mono-directional along the cylinder axis. The source particles have an initial energy of 3.2 MeV. Particles with energies less than 0.15 MeV are immediately absorbed. This energy cutoff is equivalent to all nuclides becoming pure absorbers with an infinite cross section at energies less than 0.15 MeV. Due to the simplified collision physics, the energy distribution of photons crossing any surface or volume can be calculated analytically, as well as the number of collisions in a cell and pulse-height distribution in both detector regions.

In a radiation detector, a voltage pulse is generated by the energy (charge) deposited by a single particle history and all it's progeny. The probability of each possible pulse-height for a region using the collision physics in figure 2 can be analytically determined. The pulse-height tally, or F8 tally as it is referred to in MCNP, calculates the energy pulse distribution

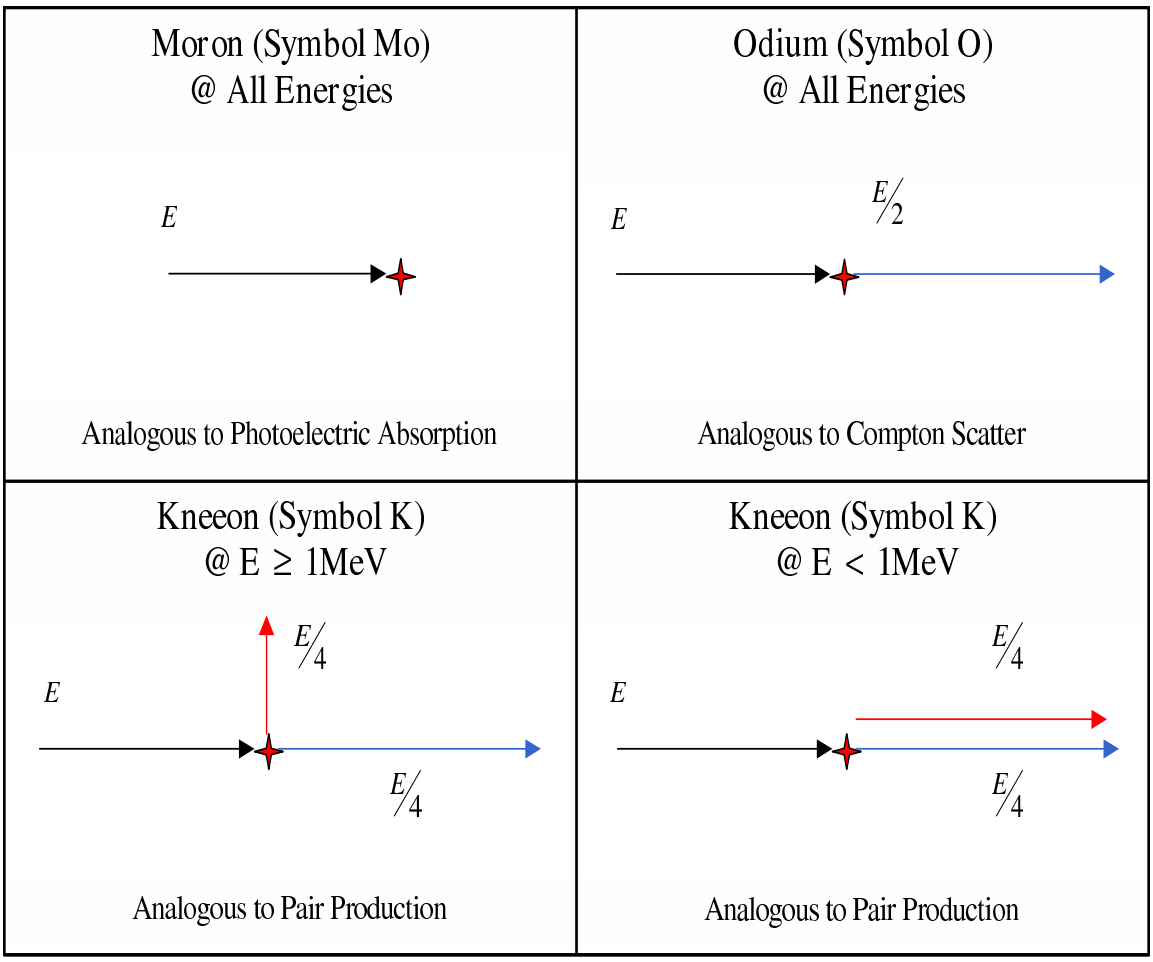

Figure 1: Collision Physics for the Three Nuclides

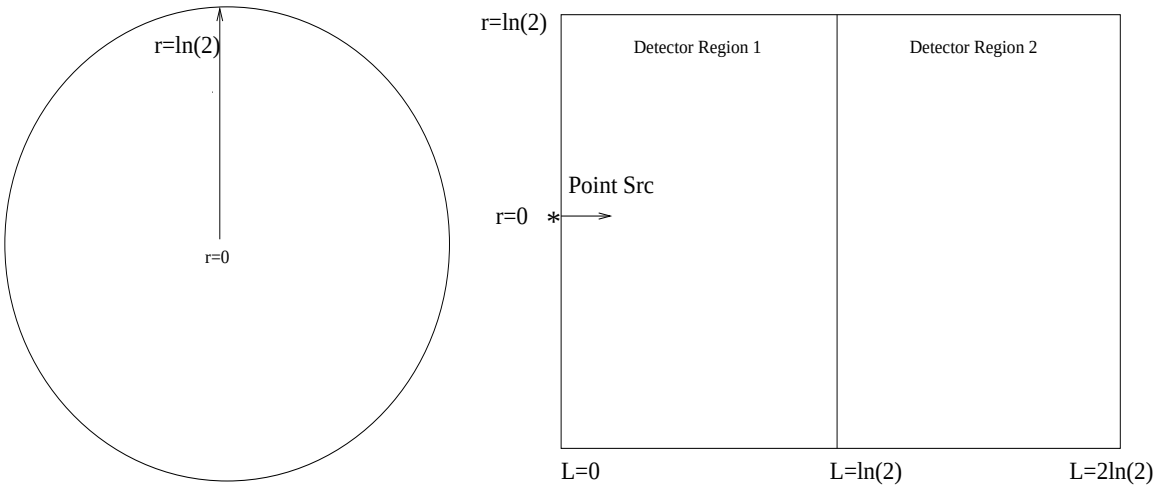

Figure 2: Two-Region Cylindrical Detector Geometry for Analytic Pulse-Height Tally Problem

deposited in a radiation detector. This tally is unique because the entire particle history myst be completed before the energy deposited can be recorded. MCNP accrues this tally by adding any particle energy that enters the cell and subtracting any particle energy leaving the cell. The summation over the history can cause complications in cases where progeny are created (e.g. pair production or double x-ray fluorescence) and when variance reduction is used, changing the weight of a particle during the random walk. As these computed pulses accumulate with more and more source particles, a probability distribution is generated by MCNP which gives the frequency for the occurance of each pulse.

Figures 3 and 4 represents all possible collisions from the 3.2 MeV source in the first cylindrical region using the collisional physics in figure 1. The top-most level on the tree represents the source. Figure 3 groups the possible particle histories by energy and figure 4 groups the possible particle histories by collision event. As shown in the interaction key in the figures, a source particle incident on a detector face suffers a number of collisions:

1. The particle may collide with a kneeon atom (the blue path),
2. The particle may exit the detector without collision (the green path),
3. The particle may collide with a moron atom and be absorbed (the red path)
4. The particle may collide with an odium atom (the yellow path)

The event trees continue for collisions with kneeon or odium, but terminates by absorption for an interaction with moron. The event trees terminate in a green arrow indicating that the particle has left a cylindrical detector region either radially or axially. This process continues and sketches out the entire trees shown in figures 3 and 4. If the source particle collides several times, it looses sufficient energy such that further collisions cause it to scatter below the energy cutoff. For particles of energy slightly above the imposed energy cutoff of 0.15 MeV, any interaction results in absorption and is represented as a single magenta line in the event tree. In all cases, a line terminating in an inverted "T" represents the absorption of a particle.

The multiplying nature of a collision with kneeon makes it possible to create several concurrent particles and further complicate the history by producing a combination of up to two axial and/or two radial particles. An example of this scenario may be seen by considering a source particle of energy 3.2 MeV that collides with kneeon giving one forward scattered particle and one radially scattered particle. This event creates two particles making a complete history consist of a particle moving in the *radial* direction and a second particle moving in the *axial* direction. For particles of energy less than 1 MeV, a kneeon interaction produces two particles, each forward-scattered. The event trees appropriately label both branches *fwd* to indicate this multiplying event.

Using figures 3 and 4, the total number of unique histories within detector region one can be determined by counting the tree branches, paying particular attention to the correlated particle scenarios. There are 40 unique histories for particles whose first interaction is not with kneeon. There are 11 possibilities for both radial and axial tracks ater an initial kneeon event. The number of unique histories is the product of the number of axial particles with the number of radial particles ($11^2 = 121$) for scenarios that collide initially with kneeon. This gives exactly 161 unique histories within detector region one. The analysis of the two region scenario proceeds in a similar fashion but is more complicated since there are five possible incident sources energies.

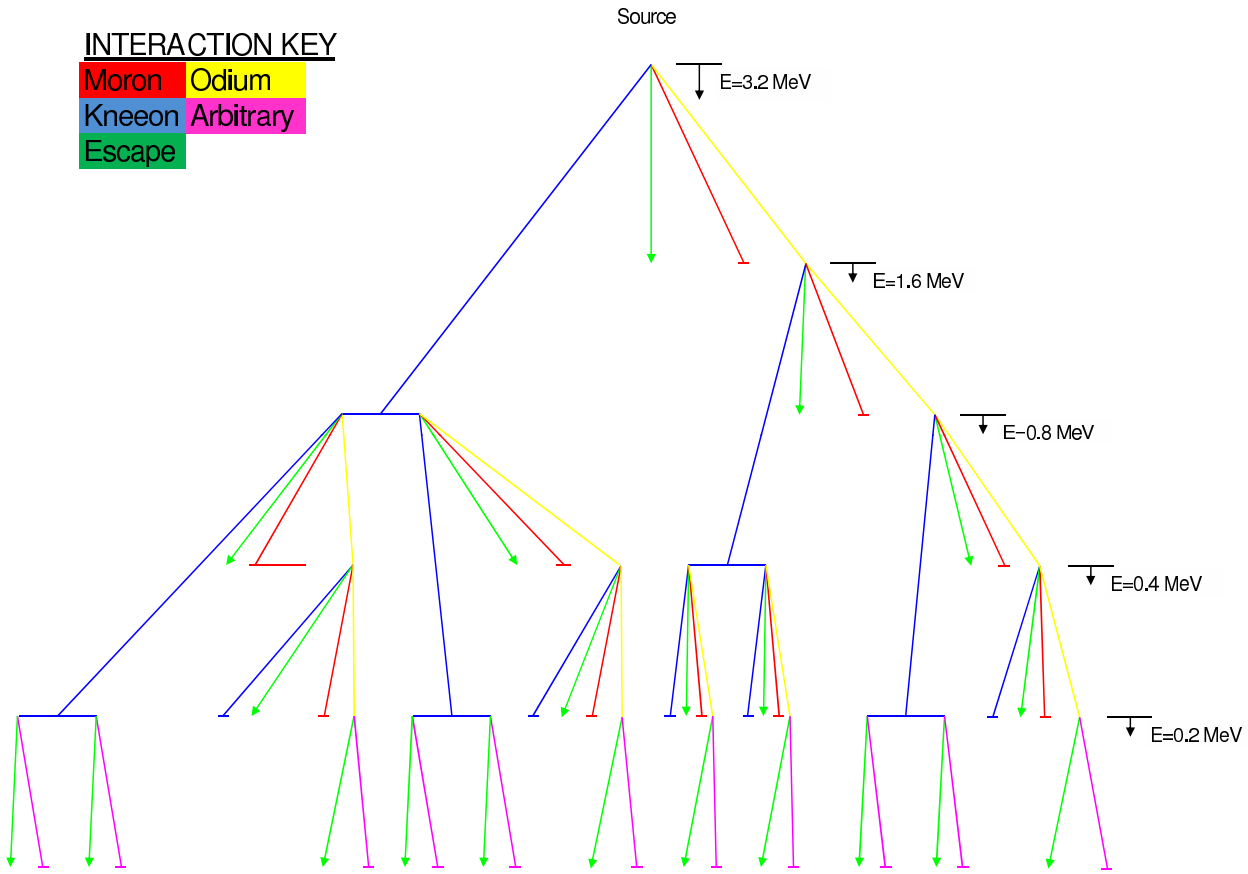

Figure 3: Energy Event Tree of up to Five Possible Energies in the Analytic Problem

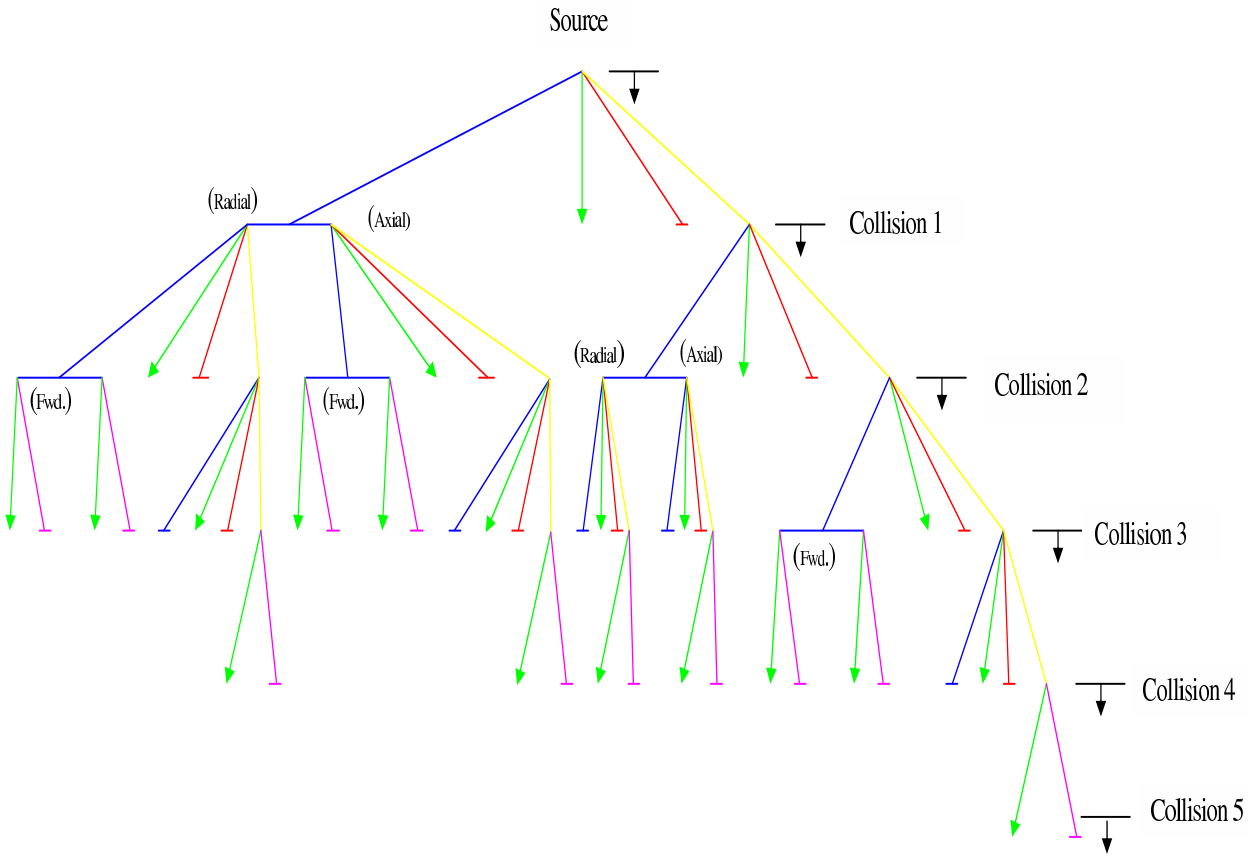

Figure 4: Collision Event Tree of up to Five Possible Axial and Four Possible Radial Collisions in the Analytic Problem

Components of The Analytic Solution

The photon collision physics description in figure 1 has been intentionally simplified from a realistic description of photon collisions to give a limited set of possible outcomes that allows the probabilities of all possible outcomes to be analytically derived. The following discussion gives the components of the equations used to generate the complete analytic solution. The multiplying interactions with kneeon are special cases that are discussed separately. The analytic solutions have been derived using the scattering, absorption, and total cross sections defined for the fictious nuclides as:

$$\begin{aligned} \Sigma_s &= \Sigma_{odium} + \Sigma_{kneeon} \\ \Sigma_a &= \Sigma_{moron} + \text{all collisions below 0.15 MeV} \\ \Sigma_t &= \Sigma_s + \Sigma_a \end{aligned}$$

Analytic pulse-height distributions require calculating the probability of each specific set of events (a history) and the total energy deposited in the cell. The components of the probabilities and average track-lengths for the possible collisions are derived below.

The probability of a single collision event, p_{coll}, in one detector region between two arbitrary points a and b is:

$$\boxed{p_{coll} = \int_a^b \exp(-\Sigma_t x)\Sigma_t dx} \tag{1}$$

$$= [\exp(-\Sigma_t a) - \exp(-\Sigma_t b)]$$

where $\exp(-\Sigma_t x)$ is the probability of traveling a distance x without collision and $\Sigma_t dx$ is the probability of a collision in dx. The collision can happen anywhere in the interval $(a, b]$. Equation 1 does not consider whether the collision was an absorption or scattering collision. The equation would be multiplied by the scattering probability, $\frac{\Sigma_s}{\Sigma_t}$, for a scattering collision or by the absorption probability, $\frac{\Sigma_a}{\Sigma_t}$, if the collision were an absorption. For $a = 0$ and $b = L$, the length of the detector region, p_{coll} reduces to: $1 - \exp(-\Sigma_t L)$ and the probability for escape, p_{esc}, becomes $\exp(-\Sigma_t L)$.

The volumetric flux can be described by the average track-length divided by the cell volume. The average track-length for a particle undergoing a single collision between points a and b , $< T_L(1) >$,:

$$\boxed{< T_L(1) > = \frac{\int_a^b x \exp(-\Sigma_t x)\Sigma_t dx}{\int_a^b \exp(-\Sigma_t x)\Sigma_t dx}} \tag{2}$$

$$= \frac{\exp(-\Sigma_t a)(\Sigma_t a + 1) - \exp(-\Sigma_t b)(\Sigma_t b + 1)}{\Sigma_t [\exp(-\Sigma_t a) - \exp(-\Sigma_t b)]}$$

For $a = 0$ and $b = L$, equation 2 reduces to the expression:

$$< T_L(1) > \quad = \quad \frac{1 - \exp(-\Sigma_t L)\,[1 + \Sigma_t L]}{\Sigma_t(1 - \exp(-\Sigma_t L))}$$

As the detector length, L approaches infinity, $< T_L >$ approaches the mean free path, $1/\Sigma_t$. Equation 2 is equivalent to the average distance *between* collisions.

Example 1: Multiple scatterings followed by escape

The previous set of equations were general and did not specifically consider the collision type (e.g. scattering or absorption). One of the common interactions to consider includes multiple scattering followed by an escape.

Probability of escaping after n collisions:

Equation 1 can be used as a basis to examine the case of two scattering collisions at arbitrary points a and b followed by an escape at L, the end of the detector cylinder, as shown in figure 5.

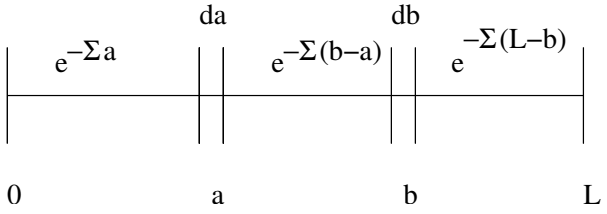

Figure 5: Collisions at a and b followed by an escape

Figure 5 shows the distances between each collision and can be used to break the problem into the product of two probablities at a, P_a, and b given that a collision occured at a followed by escape, $P_{b(a)}$.

Using equation 1, the probability of a scattering collision at point a between 0 and L is:

$$P_a \quad = \quad \frac{\Sigma_s}{\Sigma_t} \int_0^L \exp\left[-\Sigma_t a\right] \Sigma_t da$$

where $\exp\left[-\Sigma_t a\right]$ is the probability of no collision between *0* and a, and $\Sigma_t da$ is the probability of a collision in da, and $\frac{\Sigma_s}{\Sigma_t}$ is the probability of the collision being a scatter.

Similarly, the probability of having a scattering collision at point b between points a and L with the particle escaping at L is:

$$P_{b(a)} \quad = \quad \frac{\Sigma_s}{\Sigma_t} \int_a^L \exp\left[-\Sigma_t(b-a)\right] \exp\left[-\Sigma_t(L-b)\right] \Sigma_t db$$

where $\exp\left[-\Sigma_t(b-a)\right]$ is the probability of no collision between a and b, $\Sigma_t db$ is the probability of collision in db, $\frac{\Sigma_s}{\Sigma_t}$ is the probability of scattering, and $\exp\left[-\Sigma_t(L-b)\right]$ is the probability of no collision after b.

Combining both of these probablities gives the probability of escaping with two collisions between 0 and L, $p_{esc}(2)$:

$$\begin{aligned}
p_{esc}(2) &= (P_a)(P_{b(a)}) \\
&= \left(\frac{\Sigma_s}{\Sigma_t}\right)^2 \int_0^L \exp\left[-\Sigma_t a\right] \Sigma_t da \int_a^L \exp\left[-\Sigma_t (b-a)\right] \exp\left[-\Sigma_t (L-b)\right] \Sigma_t db \\
&= \left(\frac{\Sigma_s}{\Sigma_t}\right)^2 \int_0^L \exp\left[-\Sigma_t a\right] \Sigma_t \{\exp\left[-\Sigma_t (L-a)\right] (L-a)\} \Sigma_t da \\
&= \Sigma_s^2 \exp\left[-\Sigma_t L\right] \int_0^L (L-a) da \\
&= \frac{(\Sigma_s L)^2}{2} \exp\left[-\Sigma_t L\right]
\end{aligned}$$

Similarly, the probability of a particle reaching the detector length, L, having three scattering collisions at arbitrary points a, b, and c becomes:

$$\begin{aligned}
p_{esc}(3) &= \left(\frac{\Sigma_s}{\Sigma_t}\right)^3 \int_0^L \exp\left[-\Sigma_t a\right] \Sigma_t da \int_a^L \exp\left[-\Sigma_t (b-a)\right] \Sigma_t db \\
&\quad \int_b^L \exp\left[-\Sigma_t (c-b)\right] \exp\left[-\Sigma_t (L-c)\right] \Sigma_t dc \\
&= \frac{(\Sigma_s L)^3}{6} \exp\left[-\Sigma_t L\right]
\end{aligned}$$

These equations can be generalized for n collisions. The probability of incurring exactly n collisions along a path L within the detector and escaping the detector, $p_{esc}(n)$, is:

$$\boxed{p_{esc}(n) = \frac{(\Sigma_s L)^n \exp(-\Sigma_t L)}{n!}} \tag{3}$$

As the detector length, L, approaches infinity, the probability of escape approaches zero. Equation 3 assumes multiple scattering with a single nuclide. Scattering with a mixture nuclides will change Σ_s to the scattering cross section for that particular nuclide.

Average track-length:

Following equation 2, the average track-length, $< T_L(2) >_{esc}$, for two scattering collisions at points a and b followed by an escape at L is given by:

$$\begin{aligned}
< T_L(2) >_{esc} &= \frac{\left(\frac{\Sigma_s}{\Sigma_t}\right)^2 \int_0^L a \exp\left[-\Sigma_t a\right] \Sigma_t da \int_a^L \exp\left[-\Sigma_t (b-a)\right] \exp\left[-\Sigma_t (L-b)\right] \Sigma_t db}{\left(\frac{\Sigma_s}{\Sigma_t}\right)^2 \int_0^L \exp\left[-\Sigma_t a\right] \Sigma_t da \int_a^L \exp\left[-\Sigma_t (b-a)\right] \exp\left[-\Sigma_t (L-b)\right] \Sigma_t db} \\
&= \frac{\int_0^L a \exp\left[-\Sigma_t a\right] \Sigma_t \left[\Sigma_t \exp(-\Sigma_t (L-a))(L-a)\right] da}{\int_0^L \exp\left[-\Sigma_t a\right] \Sigma_t \left[\Sigma_t \exp(-\Sigma_t (L-a))(L-a)\right] da} \\
&= = \frac{(\Sigma_t)^2 \exp(-\Sigma_t L)(L^3/6)}{(\Sigma_t)^2 \exp(-\Sigma_t L)(L^2/2)} \\
< T_L(2) >_{esc} &= \frac{L}{3}
\end{aligned}$$

The equation for the average track-length for after n collisions followed by an escape at L can be generalized to:

$$\boxed{< T_L(n) >_{esc} = \frac{L}{n+1}} \tag{4}$$

As the detector length, L, approaches infinity, $< T_L >$ approaches infinity with the probability of the event approaching zero.

Example 2: Multiple scattering followed by absorption

The previous set of equations only considered scattering reactions but not absorption reactions. Another set of interactions to consider includes multiple scattering followed by an absorption.

Probability of absorption after n collisions:

Equation 1 can be used as a basis to calculate the probability of undergoing one scattering collision at point a between points 0 and L followed by an absorption at point b between points a and L, $p_{abs}(2)$, becomes:

$$\begin{aligned} p_{abs}(2) &= \int_0^L \frac{\Sigma_s}{\Sigma_t} \exp(-\Sigma_t a)\Sigma_t da \int_a^L \frac{\Sigma_a}{\Sigma_t} \exp\left[-\Sigma_t(b-a)\right]\Sigma_t db \\ &= \frac{\Sigma_a \Sigma_s}{(\Sigma_t)^2}\left[1 - \exp(-\Sigma_t L)(1-\Sigma_t L)\right] \end{aligned}$$

Stated differently, the particle will undergo $(n-1)$ scattering collisions and is absorbed on the n^{th} collision.

Similarly, the probability of having two scattering collisions at points a and b followed by an absorption at point c, $p_{abs}(3)$, is:

$$\begin{aligned} p_{abs}(3) &= \int_0^L \frac{\Sigma_s}{\Sigma_t} \exp(-\Sigma_t a)\Sigma_t da \int_a^L \frac{\Sigma_s}{\Sigma_t} \exp(-\Sigma_t(b-a))\Sigma_t db \int_b^L \frac{\Sigma_a}{\Sigma_t} \exp(-\Sigma_t(c-b))\Sigma_t dc \\ &= \left(\frac{\Sigma_a \Sigma_s^2}{\Sigma_t^3}\right) \frac{2 - \exp(-\Sigma_t L)\left[(L\Sigma_t)^2 - 2L\Sigma_t - 2\right]}{2} \\ &= \left(\frac{\Sigma_a \Sigma_s^2}{\Sigma_t^3}\right) \frac{\exp(-\Sigma_t L)\left[2\exp(\Sigma_t L) - (L\Sigma_t)^2 - 2L\Sigma_t - 2\right]}{2} \end{aligned}$$

This equation is very similar to the equation for p_{esc} except that the escape probability from collision at point c is not included.

Similarly, the equation for (n-1) collisions with an absorption on the n^{th} collision can be generalized to:

$$\boxed{p_{abs}(n) = \left(\frac{\Sigma_a \Sigma_s^{n-1}}{\Sigma_t^n}\right) \frac{\exp(-\Sigma_t L)\left[(n-1)!\exp(-\Sigma_t L) - (\Sigma_t L)^{(n-1)} - (n-1)(\Sigma_t L)^{n-2} - (n-1)(n-2)(\Sigma_t L)^{n-3}...\right]}{(n-1)!}} \tag{5}$$

Note that for $n = 1$, which represents an absorption on the first collision, equation 5 becomes: $\frac{\Sigma_a}{\Sigma_t}\left[1 - \exp(-\Sigma_t L)\right]$ and is similar to equation 1 multiplied by the probability of absorption.

Average track-length:

Following equation 2, the average track-length for two scattering collisions at points a and b followed by an absorption at point c, $< T_L(3) >_{abs}$, is:

$$\begin{aligned}
< T_L(3) >_{abs} &= \frac{\int_0^L a\frac{\Sigma_s}{\Sigma_t}\exp(-\Sigma_t a)\Sigma_t da \int_a^L \frac{\Sigma_s}{\Sigma_t}\exp(-\Sigma_t(b-a))\Sigma_t db \int_b^L \frac{\Sigma_a}{\Sigma_t}\exp(-\Sigma_t(c-b))\Sigma_t dc}{\int_0^L \frac{\Sigma_s}{\Sigma_t}\exp(-\Sigma_t a)\Sigma_t da \int_a^L \frac{\Sigma_s}{\Sigma_t}\exp(-\Sigma_t(b-a))\Sigma_t db \int_b^L \frac{\Sigma_a}{\Sigma_t}\exp(-\Sigma_t(c-b))\Sigma_t dc} \\
&= \left(\frac{1}{\Sigma_t}\right)\frac{6\exp(-\Sigma_t L) + (L\Sigma_t)^3\exp(-\Sigma_t L) + 3(L\Sigma_t)^2\exp(-\Sigma_t L) + 6(L\Sigma_t)\exp(-\Sigma_t L) - 6}{6\exp(-\Sigma_t L) + +3(L\Sigma_t)^2\exp(-\Sigma_t L) + 6(L\Sigma_t)\exp(-\Sigma_t L) - 6} \\
&= \left(\frac{1}{\Sigma_t}\right)\frac{6\exp(\Sigma_t L) - (L\Sigma_t)^3 - 3(L\Sigma_t)^2 - 6(L\Sigma_t) - 6}{6\exp(\Sigma_t L) - 3(L\Sigma_t)^2 - 6(L\Sigma_t) - 6} \\
&= \frac{1}{\Sigma_t}\left[1 - \frac{(\Sigma_t L)^3}{6\exp(\Sigma_t L) - 3(L\Sigma_t)^2 - 6(L\Sigma_t) - 6}\right]
\end{aligned}$$

Similarly, the equation for the track-length for (n-1) collisions with an absorption on the n^{th} collision can be generalized to:

$$< T_L(n) >_{abs} = \frac{1}{\Sigma_t}\left[1 - \frac{L^n}{n!\exp(\Sigma_t L) - n(\Sigma_t L)^{(n-1)} - (n-1)(n)\left[(\Sigma_t L)^{(n-2)} + 1\right] - ...}\right] \quad (6)$$

As L approaches infinity, $< T_L(n) >_{abs}$ approaches $1/\Sigma_t$.

Surface Current and Flux

Equations 3 through 6 are used in calculating the pulse-height and volumetric flux distribution. The outward current, J_+, for any particle crossing any boundary can be calculated as:

$$J_+ = \sum_1^n p_{esc}(n)$$

The number of terms n for the axial current is four and the radial current is 3. The surface flux, ϕ, can be calculated for any particle crossing any boundary as:

$$\phi = J_+/\text{surface area}$$

Example 3: A Complete Example History

Figure 6 is a complete event from Shuttleworth's paper [5] and uses the collisional physics in figure 1. This event is one of the 161 unique possible histories within detector region one. In this example, a particle begins with an energy of 3.2 MeV. It first collides with kneeon (pair production), which creates two particles with energy 0.8 MeV, and scatters one particle axially and one particle radially. The radial particle collides with moron (photoelectric) and is fully absorbed depositing 0.8 Mev in the detector region. The axial particle collides with

odium (Compton scatter), is reduced to 0.4 MeV, and escapes. The complete event deposits 2.8 MeV inside the cell and 0.4 MeV escapes the right hand side.

The pulse-height tally can be calculated by determining the total probability of this history, P(history), and is the combined probability of both radial and axial events. This probability is equal to:

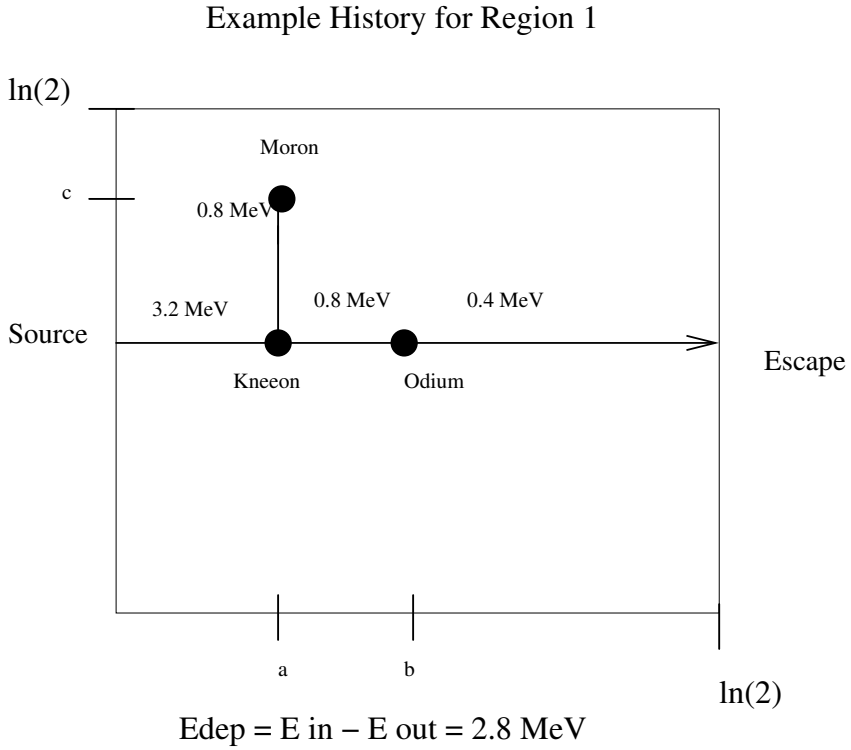

Figure 6: Sample History for Example 3

$$P(\text{history}) = P_{\text{radial}} P_{\text{axial}}$$

The probability for the radial event, P_{radial}, can be calculated using equation 5 for n=1. P_{radial} becomes:

$$\begin{aligned} P_{\text{radial}} &= p_{abs}(1) \\ &= \left(\frac{\Sigma_a}{\Sigma_t}\right)[1 - \exp(-\Sigma_t L)] \\ &= (0.2)\,[1 - \exp(-\ln(2))] \\ P_{\text{radial}} &= 0.1 \end{aligned}$$

The probability for the axial event, P_{axial}, can be calculated using equation 3 for $n = 2$. P_{axial} becomes:

$$\begin{aligned} P_{\text{axial}} &= p_{esc}(2) \\ &= \frac{(\Sigma_{kneeon}\Sigma_{odium})L^2 \exp(-\Sigma_t L)}{2} \end{aligned}$$

$$
\begin{aligned}
&= \frac{(0.5)(0.3)(\ln(2))^2 \exp(-\ln(2)))}{2} \\
P_{\text{axial}} &= 0.018016988
\end{aligned}
$$

The probability for the example history is:

$$
\begin{aligned}
P(\text{history}) &= P_{\text{radial}} P_{\text{axial}} \\
&= 0.0018016988
\end{aligned}
$$

This history occurs with probability $P(\text{history})$ and produces a pulse of 2.8 MeV.

The average track-length for this event can be similarly calculated using equations 4 and 6. The average track-length must be calculated for each distance traveled between collisions and grouped corresponding to the particle's energy at the start of the track.

The track-length at 3.2 MeV is:

$$
\begin{aligned}
< T_L >_{3.2 \text{ MeV}} &= < T_L(2) >_{esc} \\
&= \frac{L}{3} \\
&= \frac{\ln(2)}{3} \\
< T_L >_{3.2 \text{ MeV}} &= 0.23104906
\end{aligned}
$$

The track-length at 0.8 MeV is:

$$
\begin{aligned}
< T_L >_{0.8 \text{ MeV}} &= < T_L(2) >_{esc} + < T_L(1) >_{abs} \\
&= \frac{L}{3} + \left(\frac{1}{\Sigma_t}\right)\left[1 - \frac{L}{\exp(\Sigma_t L) - 1}\right] \\
&= \frac{\ln(2)}{3} + \left[1 - \frac{\ln(2)}{\exp(\ln(2)) - 1}\right] \\
< T_L >_{0.8 \text{ MeV}} &= 0.53790188
\end{aligned}
$$

The track-length at 0.4 MeV is:

$$
\begin{aligned}
< T_L >_{0.4 \text{ MeV}} &= < T_L(2) >_{esc} \\
&= \frac{L}{3} \\
&= \frac{\ln(2)}{3} \\
< T_L >_{0.4 \text{ MeV}} &= 0.23104906
\end{aligned}
$$

The current and surface flux can be calculated for the single particle escaping along the axis. The current and surface flux are:

$$
\begin{aligned}
J_+ &= p_{esc}(2) \\
&= \frac{(\Sigma_{kneeon}\Sigma_{odium}) L^2 \exp(-\Sigma_t L)}{2}
\end{aligned}
$$

$$
\begin{aligned}
&= \frac{(0.5)(0.3)(\ln(2))^2 \exp(-\ln(2)))}{2} \\
J_+ &= 0.018016988
\end{aligned}
$$

$$
\begin{aligned}
\phi &= \frac{J_+}{\pi \ln(2)^2} \\
\phi &= 0.01193662
\end{aligned}
$$

Special Case: Correlated progeny (Kneeon)

Special care must be taken for generating the interaction probabilities for the correlated kneeon (pair production) event. There are five possible collisions with kneeon (pair production). Within each of these possible collision with kneeon there are three additional possible outcomes for the progeny created. Unlike the general description for p_{abs} and p_{esc}, there is no general way to describe these collisions. Each of the five possible collisions with kneeon require specific examination replace the equations 3 through 6.

Generation of High-Precision Results

A computer code was written to calculate the probabilities of all possible histories[7, 8]*. An indexing scheme was developed that uniquely identified the all collisions in a history. This indexing scheme ensured that the probabilities and energy losses for all possible collisions were calcuated and that none were missed. Many quantities could be easily checked to verify the computer code was correct (e.g. the probability that a particle escapes the first region is 0.5, the sum of all probabilities is unity, etc).

Any particle escaping the first region axially was considered to be a source particle for the second region. The probability of escaping the cylinder and escape energy was recorded and used to generate a subsequent source (instead of 3.2 MeV with probability of 1.0) for the next cylinder. The subsequent probabilities (pulse-heights, volumetric fluxes, currents, etc) for the second cylinder were multiplied by the probability of the original source particle escaping the first cylinder.

*M.S. Reed (Nuclear Engineering Dept., Texas A&M University) generated all high-precision numerical results presented here as a part of his summer project at LANL (2003,2004). Only a few results were published.

Numerical Results

Tables 1 through 4 give the numerical results for the photon leakage currents, surface fluxes, volume fluxes, and pulse-height distribution for both cylinders. Ten digits of precision are reported for photon surface and volume fluxes and pulse-height tallies. Six digits of precision are reported for the total photon leakage currents. These values were generated exactly, with no approximations and are only limited by computer precision.

TABLE 1: Total Photon Leakage Current

Region	J_+(axial)	J_+(radial)
1	0.889943	0.254239
2	0.764351	0.142818

TABLE 2: Photon Surface Flux

Energy (MeV)	Diameter Region 1 Surface flux ($1/cm^2$)	Diameter Region 2 Surface flux ($1/cm^2$)	Energy (MeV)	Axis Region 1 Surface flux ($1/cm^2$)	Axis Region 2 Surface flux ($1/cm^2$)
0.20	0.0303893949	0.0160899440	0.20	0.0431240772	0.0930220670
0.40	0.0124222561	0.0105163539	0.40	0.0243696716	0.0497322033
0.80	0.0414075202	0.0207037601	0.80	0.1219679960	0.1291299684
			1.60	0.0688836141	0.0688836141
			3.20	0.3312601617	0.1656300809

TABLE 3: Photon Volume Flux

Energy (MeV)	Region 1 Volume flux ($1/cm^2$)	Region 2 Volume flux ($1/cm^2$)
0.20	0.0552739100	0.0905357642
0.40	0.0316929622	0.0618684956
0.80	0.1956661722	0.1903885628
1.60	0.0439941693	0.0716861089
3.20	0.4779073926	0.2389536963

TABLE 4: Photon Pulse-Height Distribution

Energy (MeV)	Region 1 Pulse-Height Distribution	Energy (MeV)	Region 2 Pulse-Height Distribution
0.00	0.5000000000	0.00	0.4260696364
1.60	0.1906154747	0.20	0.0237685679
2.00	0.0607580302	0.40	0.0630209469
2.20	0.0251175286	0.60	0.0197690310
2.40	0.0685966790	0.80	0.0499450801
2.60	0.0100059394	1.00	0.0028098955
2.80	0.0241757434	1.20	0.0130114830
3.00	0.0057451938	1.40	0.0021885293
3.20	0.1149854109	1.60	0.1094651813
		2.00	0.0303790151
		2.20	0.0125587643
		2.40	0.0342983395
		2.60	0.0050029697
		2.80	0.0120878717
		3.00	0.0028725969
		3.20	0.0574927055
total	1.0000000000		0.8647406141

Calculated Results for MCNP 5.1.50

MCNP can calculate pulse-heights when the source particle or progeny is a photon or electron and if both photons and electrons are being transported. However, pulse-height tallies are not valid when neutrons are being transported. The physical laws for the photon physics are hard-coded and not controllable through the cross section data unlike neutron interactions. Controlling the collisional photon physics through the data will not work. Some very simple changes were made to MCNP's subroutine, *colidp*, to implement the collision physics in figure 1.

Tables 5 - 8 compare the analytic results with analog MCNP 5.1.50 (MCNP5 LANL, 1.50.pre6) photon calculations for photon currents (F1) and surface fluxes (F2) across the cell interfaces and volume (F4) and pulse-height distributions (F8) in each cell. MCNP was run for 100 million histories giving relative errors (RE) of 0.06% or better. The MCNP calculated estimated means are reported to six digits and relative errors are reported to four digits. The last column compares differences in the MCNP calculated value and the analytic solution in terms of standard deviations (or sigma). These values are expected to follow a normal distribution with half of the values positive and half of the values negative. As with a normal distribution, sixty-eight percent of the MCNP calculated answers are expected to be within one sigma, ninety-five percent within two sigma and ninety-nine percent within three sigma. These tables show that all of MCNP's calculated values match the analytic values up to four or five significant figures with no value more than three standard deviations away from the analytic solution. The MCNP calculated answers follow the expected behaviour of a normal distribution with roughly equally half the results above and below the analytic results.

TABLE 5: Analog MCNP Total Photon Leakage Current

Location	Analytic	MCNP 5 (R.E.)	Number of S.D away
<u>Axis</u>			
Region 1	0.889943	0.889896 +/- 0.0000	0.00
Region 2	0.764351	0.764251 +/- 0.0001	-1.31
<u>Diameter</u>			
Region 1	0.254239	0.254223 +/- 0.0002	-0.31
Region 2	0.142818	0.142860 +/- 0.0003	0.98

TABLE 6: Analog MCNP Photon Surface Flux Results

Location	Energy (MeV)	Analytic	MCNP 5 (R.E.)	Number of S.D away
Axis				
Region 1	0.20	0.0431240772	0.043106 +/- 0.0005	-0.84
	0.40	0.0243696716	0.024377 +/- 0.0005	0.60
	0.80	0.1219679960	0.121936 +/- 0.0002	-1.31
	1.60	0.0688836141	0.068877 +/- 0.0003	-0.30
	3.20	0.3312601617	0.331278 +/- 0.0001	0.54
Region 2				
	0.20	0.0930220670	0.092980 +/- 0.0003	-1.52
	0.40	0.0497322033	0.049750 +/- 0.0004	0.88
	0.80	0.1291299684	0.129123 +/- 0.0002	-0.27
	1.60	0.0688836141	0.068885 +/- 0.0003	0.05
	3.20	0.1656300809	0.165595 +/- 0.0002	-1.06
Diameter				
Region 1	0.20	0.0303893949	0.030402 +/- 0.0004	1.07
	0.40	0.0124222561	0.012420 +/- 0.0005	-0.40
	0.80	0.0414075202	0.041392 +/- 0.0003	-1.25
Region 2	0.20	0.0160899440	0.016097 +/- 0.0006	0.73
	0.40	0.0105163539	0.010522 +/- 0.0006	0.95
	0.80	0.0207037601	0.020705 +/- 0.0004	0.10

TABLE 7: Analog MCNP Photon Volume Flux Results

Location	Energy (MeV)	Analytic	MCNP 5 (R.E.)	Number of S.D away
Region 1	0.20	0.0552739100	0.055267 +/- 0.0004	-0.31
	0.40	0.0316929622	0.031707 +/- 0.0004	1.08
	0.80	0.1956661722	0.195609 +/- 0.0002	-1.46
	1.60	0.0439941693	0.043989 +/- 0.0003	-0.43
	3.20	0.4779073926	0.477914 +/- 0.0000	0.00
Region 2				
	0.20	0.0905357642	0.090521 +/- 0.0003	-0.54
	0.40	0.0618684956	0.061891 +/- 0.0003	1.23
	0.80	0.1903885628	0.190389 +/- 0.0002	0.01
	1.60	0.0716861089	0.071685 +/- 0.0003	-0.05
	3.20	0.2389536963	0.238945 +/- 0.0001	-0.36

TABLE 8: Analog MCNP Photon Pulse-Height Results

Location	Energy (MeV)	Analytic	MCNP 5 (R.E.)	Number of S.D away
Region 1	total	1.125288	1.125290 +/- 0.0001	0.02
Region 2	total	0.688563	0.688757 +/- 0.0001	2.82
Region 1	0.00	0.5000000000	0.500026 +/- 0.0001	0.52
	1.60	0.1906154747	0.190560 +/- 0.0002	-1.46
	2.00	0.0607580302	0.060770 +/- 0.0004	0.49
	2.20	0.0251175286	0.025103 +/- 0.0006	-0.97
	2.40	0.0685966790	0.068608 +/- 0.0004	0.40
	2.60	0.0100059394	0.009994 +/- 0.0010	-1.19
	2.80	0.0241757434	0.024175 +/- 0.0006	-0.05
	3.00	0.0057451938	0.005749 +/- 0.0013	0.57
	3.20	0.1149854109	0.115015 +/- 0.0003	0.86
	total	1.0000000000	1.000000 +/- 0.0000	
Region 2	0.00	0.4260696364	0.425953 +/- 0.0001	-2.74
	0.20	0.0237685679	0.023765 +/- 0.0006	-0.25
	0.40	0.0630209469	0.063003 +/- 0.0004	-0.71
	0.60	0.0197690310	0.019774 +/- 0.0007	0.34
	0.80	0.0499450801	0.049939 +/- 0.0004	-0.32
	1.00	0.0028098955	0.002813 +/- 0.0019	0.65
	1.20	0.0130114830	0.013023 +/- 0.0009	0.94
	1.40	0.0021885293	0.002190 +/- 0.0021	0.36
	1.60	0.1094651813	0.109498 +/- 0.0003	1.00
	2.00	0.0303790151	0.030382 +/- 0.0006	0.15
	2.20	0.0125587643	0.012574 +/- 0.0009	1.37
	2.40	0.0342983395	0.034307 +/- 0.0005	0.48
	2.60	0.0050029697	0.005002 +/- 0.0014	-0.20
	2.80	0.0120878717	0.012117 +/- 0.0009	2.70
	3.00	0.0028725969	0.002874 +/- 0.0019	0.20
	3.20	0.0574927055	0.057490 +/- 0.0004	-0.12
	total	0.8647406141	0.864703 +/- 0.0000	

Analytic Verification of MCNP 5.1.50 Pulse-Height-Tally with Variance Reduction

Analytic Verification of MCNP 5.1.50 Pulse-Height-Tally with Variance Reduction

Prior to the release of version 5.1.50, MCNP has allowed the user to apply variance reduction techniques to all tallies except the pulse-height tally. This restriction was due to the lack of any theoretical basis for applying variance reduction for processes that depend upon the collective effects of groups of particles like the pulse-height tally. The release of MCNP 5.1.50 applies the theoretical basis given in references [2, 3] and allows MCNP users to apply variance reduction for photon and photon/electron mode problems. This new approach is complex because an entire history "tree" must be recorded and analyzed to properly combine all the energy deposited into a single pulse-height.

This new complex feature was verified by comparing MCNP 5.1.50 (MCNP5 LANL, 1.50.pre6) calculated results using many of the variance reduction techniques available with the analytic solution given in tables 1 - 4. MCNP users can apply each of the variance reduction techniques listed in table 9 or in combination. Most of these techniques were tested individually with many of them in combination. Table 10 summarizes the variance reduction techniques tested as a part of this work. Calculated results were generated for photon currents and surface fluxes across detector cell interfaces and volume flux and pulse-height energy distributions in each detector cell. These results were intentionally generated in a single calculation to verify that the new feature correctly calculated both Boltzmann-type flux tallies and the pulse-height tally using variance reduction in the same problem.

TABLE 9: Photon Variance Reduction Techniques Available

Geometry / Energy / Time splitting with Roulette
Weight Window
Exponential Transform
Forced Collision
Implicit Capture / Weight Cutoff
DXTRAN
Source Biasing

TABLE 10: Photon Variance Reduction Techniques Tested

Geometry Splitting / Russian Roulette
Geometry Splitting / Russian Roulette off
Implicit Capture / Weight Cutoff
Wgt Windows (generation)
Weight Windows usage
Weight Windows + Forced Collision
Weight Windows + Exponential Transform

Comparison of the Analytic Solutions with MCNP 5.1.50 Calculated Results for Photon Transport with Variance Reduction

MCNP calculated results were generated on LANL's Linux cluster (Yellow-Rail) which has four dual-core AMD opteron 64-bit processors running at 2.2 GHz. All eight CPUs share 32 GBytes of RAM and are running RedHat Enterprise Linux 4. MCNP 5.1.50 (MCNP5 LANL, 1.50.pre6) was executed using MPI for message passing and OpenMP for threading on 16 processors with 2 threads each. The numerical results are given in tables 11 through 34. These results were generated using photon transport only and do not include secondary photon particles (e.g. bremsstrahlung, x-rays, fluorescence, etc). All MCNP calculated results match the analytic solutions to four or five significant figures and are normally distributed. There are a few results with relative errors of zero or standard deviations greater than two. The 'number of SD away' values are considered to be unreliable since the relative error is printed out to only five decimal places.

Results: Analog with History Tree Structure

Tables 11 through 14 compare the analytic results with MCNP 5.1.50 results run in analog mode but forced the use of the "tree" structure that was created to track the various variance reduction branches (dbcn 22j 1). These tables are identical to tables 5 through 8

TABLE 11: Analog MCNP Total Photon Leakage Current

Location	Analytic	MCNP 5 (R.E.)	Number of S.D away
<u>Axis</u>			
Region 1	0.889943	0.889896 +/- 0.0000	0.00
Region 2	0.764351	0.764251 +/- 0.0001	-1.31
<u>Diameter</u>			
Region 1	0.254239	0.254223 +/- 0.0002	-0.31
Region 2	0.142818	0.142860 +/- 0.0003	0.98

TABLE 12: Analog MCNP Photon Surface Flux Results

Location	Energy (MeV)	Analytic	MCNP 5 (R.E.)	Number of S.D away
Axis				
Region 1	0.20	0.0431240772	0.04310600 +/- 0.0005	-0.84
	0.40	0.0243696716	0.02437700 +/- 0.0005	0.60
	0.80	0.1219679960	0.12193600 +/- 0.0002	-1.31
	1.60	0.0688836141	0.06887740 +/- 0.0003	-0.30
	3.20	0.3312601617	0.33127800 +/- 0.0001	0.54
Region 2				
	0.20	0.0930220670	0.09297970 +/- 0.0003	-1.52
	0.40	0.0497322033	0.04974970 +/- 0.0004	0.88
	0.80	0.1291299684	0.12912300 +/- 0.0002	-0.27
	1.60	0.0688836141	0.06888460 +/- 0.0003	0.05
	3.20	0.1656300809	0.16559500 +/- 0.0002	-1.06
Diameter				
Region 1	0.20	0.0303893949	0.03040240 +/- 0.0004	1.07
	0.40	0.0124222561	0.01241980 +/- 0.0005	-0.40
	0.80	0.0414075202	0.04139200 +/- 0.0003	-1.25
Region 2	0.20	0.0160899440	0.01609700 +/- 0.0006	0.73
	0.40	0.0105163539	0.01052240 +/- 0.0006	0.96
	0.80	0.0207037601	0.02070460 +/- 0.0004	0.10

TABLE 13: Analog MCNP Photon Volume Flux Results

Location	Energy (MeV)	Analytic	MCNP 5 (R.E.)	Number of S.D away
Region 1	0.20	0.0552739100	0.0552671 +/- 0.0004	-0.31
	0.40	0.0316929622	0.0317066 +/- 0.0004	1.08
	0.80	0.1956661722	0.1956090 +/- 0.0002	-1.46
	1.60	0.0439941693	0.0439885 +/- 0.0003	-0.43
	3.20	0.4779073926	0.4779140 +/- 0.0000	0.00
Region 2				
	0.20	0.0905357642	0.0905211 +/- 0.0003	-0.54
	0.40	0.0618684956	0.0618914 +/- 0.0003	1.23
	0.80	0.1903885628	0.1903890 +/- 0.0002	0.01
	1.60	0.0716861089	0.0716851 +/- 0.0003	-0.05
	3.20	0.2389536963	0.2389450 +/- 0.0001	-0.36

TABLE 14: Analog MCNP Photon Pulse-Height Results

Location	Energy (MeV)	Analytic	MCNP 5 (R.E.)	Number of S.D away
Region 1	total	1.125288	1.125290 +/- 0.0001	0.02
Region 2	total	0.688563	0.688757 +/- 0.0001	2.82
Region 1	0.00	0.5000000000	0.50002600 +/- 0.0001	0.52
	1.60	0.1906154747	0.19056000 +/- 0.0002	-1.46
	2.00	0.0607580302	0.06076990 +/- 0.0004	0.49
	2.20	0.0251175286	0.02510290 +/- 0.0006	-0.97
	2.40	0.0685966790	0.06860770 +/- 0.0004	0.40
	2.60	0.0100059394	0.00999403 +/- 0.001	-1.19
	2.80	0.0241757434	0.02417500 +/- 0.0006	-0.05
	3.00	0.0057451938	0.00574948 +/- 0.0013	0.57
	3.20	0.1149854109	0.11501500 +/- 0.0003	0.86
	total	1.0000000000	1.00000000 +/- 0.0000	0.00
Region 2	0.00	0.4260696364	0.42595300 +/- 0.0001	-2.74
	0.20	0.0237685679	0.02376500 +/- 0.0006	-0.25
	0.40	0.0630209469	0.06300310 +/- 0.0004	-0.71
	0.60	0.0197690310	0.01977370 +/- 0.0007	0.34
	0.80	0.0499450801	0.04993870 +/- 0.0004	-0.32
	1.00	0.0028098955	0.00281337 +/- 0.0019	0.65
	1.20	0.0130114830	0.01302250 +/- 0.0009	0.94
	1.40	0.0021885293	0.00219019 +/- 0.0021	0.36
	1.60	0.1094651813	0.10949800 +/- 0.0003	1.00
	2.00	0.0303790151	0.03038180 +/- 0.0006	0.15
	2.20	0.0125587643	0.01257430 +/- 0.0009	1.37
	2.40	0.0342983395	0.03430650 +/- 0.0005	0.48
	2.60	0.0050029697	0.00500156 +/- 0.0014	-0.20
	2.80	0.0120878717	0.01211730 +/- 0.0009	2.70
	3.00	0.0028725969	0.00287371 +/- 0.0019	0.20
	3.20	0.0574927055	0.05748990 +/- 0.0004	-0.12
	total	0.8647406141	0.86470300 +/- 0.0000	0.00

Results: Geometry Splitting

Tables 15 through 18 compare MCNP 5.1.50 calculated results using non-integer geometry splitting with Russian Roulette turned off. The two cylinders were sub-divided into 10 smaller cylinders along the axis. Each of these new cells' importances were specified such that the ratio of neighboring cell importances was not an integer value nor were always increasing. This was intentionally done to stress the geometry splitting and Russian Roulette capabilities.

TABLE 15: Geometry Splitting MCNP Total Photon Leakage Current

Location	Analytic	MCNP 5 (R.E.)	Number of S.D away
Axis			
Region 1	0.889943	0.889948 +/- 0.0000	0.00
Region 2	0.764351	0.764368 +/- 0.0000	0.00
Diameter			
Region 1	0.254239	0.254206 +/- 0.0001	-1.3
Region 2	0.142818	0.142836 +/- 0.0001	1.26

TABLE 16: Geometry Splitting MCNP Photon Surface Flux Results

Location	Energy (MeV)	Analytic	MCNP 5 (R.E.)	Number of S.D away
Axis				
Region 1	0.20	0.0431240772	0.0431123 +/- 0.0002	-1.37
	0.40	0.0243696716	0.0243652 +/- 0.0002	-0.92
	0.80	0.1219679960	0.1219660 +/- 0.0001	-0.16
	1.60	0.0688836141	0.0688733 +/- 0.0001	-1.50
	3.20	0.3312601617	0.3312920 +/- 0.0001	0.96
Region 2				
	0.20	0.0930220670	0.0930154 +/- 0.0001	-0.72
	0.40	0.0497322033	0.0497329 +/- 0.0001	0.14
	0.80	0.1291299684	0.1291320 +/- 0.0001	0.16
	1.60	0.0688836141	0.0688773 +/- 0.0001	-0.92
	3.20	0.1656300809	0.1656510 +/- 0.0001	1.26
Diameter				
Region 1	0.20	0.0303893949	0.0303849 +/- 0.0003	-0.49
	0.40	0.0124222561	0.0124220 +/- 0.0003	-0.07
	0.80	0.0414075202	0.0414015 +/- 0.0002	-0.73
Region 2	0.20	0.0160899440	0.0160922 +/- 0.0001	1.40
	0.40	0.0105163539	0.0105175 +/- 0.0001	1.09
	0.80	0.0207037601	0.0207062 +/- 0.0001	1.18

TABLE 17: Geometry Splitting MCNP Photon Volume Flux Results

Location	Energy (MeV)	Analytic	MCNP 5 (R.E.)	Number of S.D away
Region 1	0.20	0.0552739100	0.0552502 +/- 0.0004	-2.15
	0.40	0.0316929622	0.0316917 +/- 0.0002	-0.20
	0.80	0.1956661722	0.1956450 +/- 0.0001	-1.08
	1.60	0.0439941693	0.0439889 +/- 0.0002	-0.60
	3.20	0.4779073926	0.4779260 +/- 0.0000	0.00
Region 2				
	0.20	0.0905357642	0.0905245 +/- 0.0001	-1.24
	0.40	0.0618684956	0.0618698 +/- 0.0001	0.21
	0.80	0.1903885628	0.1903970 +/- 0.0001	0.44
	1.60	0.0716861089	0.0716788 +/- 0.0001	-1.02
	3.20	0.2389536963	0.2389780 +/- 0.0001	1.02

TABLE 18: Geometry Splitting MCNP Photon Pulse-Height Results

Location	Energy (MeV)	Analytic	MCNP 5 (R.E.)	Number of S.D away
Region 1	total	1.125288	1.12525 +/- 0.0001	-0.3
Region 2	total	0.688563	0.68860 +/- 0.0000	0.00
Region 1	0.00	0.5000000000	0.50005200 +/- 0.0001	1.04
	1.60	0.1906154747	0.19059400 +/- 0.0001	-1.1
	2.00	0.0607580302	0.06075630 +/- 0.0002	-0.1
	2.20	0.0251175286	0.02511270 +/- 0.0003	-0.6
	2.40	0.0685966790	0.06859140 +/- 0.0002	-0.3
	2.60	0.0100059394	0.00999950 +/- 0.0005	-1.2
	2.80	0.0241757434	0.02417610 +/- 0.0003	0.05
	3.00	0.0057451938	0.00574888 +/- 0.0006	1.07
	3.20	0.1149854109	0.11499300 +/- 0.0002	0.33
	total	1.0000000000	1.00002000 +/- 0.0000	0.00
Region 2	0.00	0.4260696364	0.42609200 +/- 0.0000	0.00
	0.20	0.0237685679	0.02376300 +/- 0.0002	-1.1
	0.40	0.0630209469	0.06301050 +/- 0.0001	-1.6
	0.60	0.0197690310	0.01976760 +/- 0.0001	-0.7
	0.80	0.0499450801	0.04994390 +/- 0.0001	-0.2
	1.00	0.0028098955	0.00281024 +/- 0.0003	0.41
	1.20	0.0130114830	0.01300900 +/- 0.0002	-0.9
	1.40	0.0021885293	0.00218731 +/- 0.0003	-1.8
	1.60	0.1094651813	0.10946400 +/- 0.0001	-0.1
	2.00	0.0303790151	0.03038640 +/- 0.0001	2.43
	2.20	0.0125587643	0.01255720 +/- 0.0001	-1.2
	2.40	0.0342983395	0.03429850 +/- 0.0001	0.05
	2.60	0.0050029697	0.00500430 +/- 0.0002	1.33
	2.80	0.0120878717	0.01209050 +/- 0.0001	2.17
	3.00	0.0028725969	0.00287364 +/- 0.0003	1.21
	3.20	0.0574927055	0.05750100 +/- 0.0001	1.44
	total	0.8647406141	0.86475900 +/- 0.0000	0.00

Results: Implicit Capture and Weight Cutoff

Tables 19 through 22 compare MCNP 5.1.50 calculated results using the default implicit capture and weight cutoff variance reduction techniques. Interestingly, each collision should reduce the weight by 0.8. The maximum number of collisions with an energy greater than 0.2 MeV is four. Thus, $(0.8)^4$=0.41 is the smallest weight possible. The particle's weight continually decreases and will never increase because the weight never falls below the default weight cutoff of 0.25. Since the default value was not changed, the weight cutoff technique is never used.

TABLE 19: Impl. Capt./Wgt. Cut MCNP Total Photon Leakage Current

Location	Analytic	MCNP 5 (R.E.)	Number of S.D away
Axis			
Region 1	0.889943	0.889957 +/- 0.0000	0.00
Region 2	0.764351	0.764307 +/- 0.0000	0.00
Diameter			
Region 1	0.254239	0.254224 +/- 0.0002	-0.30
Region 2	0.142818	0.142877 +/- 0.0002	2.06

TABLE 20: Impl. Capt./Wgt. Cut MCNP Photon Surface Flux Results

Location	Energy (MeV)	Analytic	MCNP 5 (R.E.)	Number of S.D away
Axis				
Region 1	0.20	0.0431240772	0.0431329 +/- 0.0004	0.51
	0.40	0.0243696716	0.0243733 +/- 0.0004	0.37
	0.80	0.1219679960	0.1219460 +/- 0.0002	-0.90
	1.60	0.0688836141	0.0688848 +/- 0.0003	0.06
	3.20	0.3312601617	0.3312780 +/- 0.0001	0.54
Region 2				
	0.20	0.0930220670	0.0929935 +/- 0.0002	-1.50
	0.40	0.0497322033	0.0497430 +/- 0.0003	0.72
	0.80	0.1291299684	0.1291450 +/- 0.0002	0.58
	1.60	0.0688836141	0.0688925 +/- 0.0003	0.43
	3.20	0.1656300809	0.1655950 +/- 0.0002	-1.00
Diameter				
Region 1	0.20	0.0303893949	0.0303913 +/- 0.0003	0.21
	0.40	0.0124222561	0.0124084 +/- 0.0004	-2.70
	0.80	0.0414075202	0.0414148 +/- 0.0002	0.88
Region 2	0.20	0.0160899440	0.0160998 +/- 0.0005	1.22
	0.40	0.0105163539	0.0105219 +/- 0.0004	1.32
	0.80	0.0207037601	0.0207079 +/- 0.0003	0.67

TABLE 21: Impl. Capt./Wgt. Cut MCNP Photon Volume Flux Results

Location	Energy (MeV)	Analytic	MCNP 5 (R.E.)	Number of S.D away
Region 1	0.20	0.0552739100	0.0552834 +/- 0.0003	0.57
	0.40	0.0316929622	0.0316687 +/- 0.0003	-2.55
	0.80	0.1956661722	0.1956630 +/- 0.0002	-0.08
	1.60	0.0439941693	0.0439981 +/- 0.0003	0.30
	3.20	0.4779073926	0.4779140 +/- 0.0000	0.00
Region 2				
	0.20	0.0905357642	0.0905394 +/- 0.0002	0.20
	0.40	0.0618684956	0.0618727 +/- 0.0002	0.34
	0.80	0.1903885628	0.1903980 +/- 0.0001	0.50
	1.60	0.0716861089	0.0716950 +/- 0.0002	0.62
	3.20	0.2389536963	0.2389450 +/- 0.0001	-0.36

TABLE 22: Impl. Capt./Wgt. Cut MCNP Photon Pulse-Height Results

Location	Energy (MeV)	Analytic	MCNP 5 (R.E.)	Number of S.D away
Region 1	total	1.125288	1.125220 +/- 0.0001	-0.60
Region 2	total	0.688563	0.688738 +/- 0.0001	2.54
Region 1	0.00	0.5000000000	0.5000260 +/- 0.0001	0.52
	1.60	0.1906154747	0.1906180 +/- 0.0002	0.07
	2.00	0.0607580302	0.0607408 +/- 0.0003	-0.95
	2.20	0.0251175286	0.0251344 +/- 0.0005	1.34
	2.40	0.0685966790	0.0685789 +/- 0.0003	-0.86
	2.60	0.0100059394	0.0099948 +/- 0.0007	-1.59
	2.80	0.0241757434	0.0241878 +/- 0.0004	1.25
	3.00	0.0057451938	0.0057434 +/- 0.0008	-0.38
	3.20	0.1149854109	0.1149760 +/- 0.0001	-0.82
	total	1.0000000000	1.0000000 +/- 0.0000	0.00
Region 2	0.00	0.4260696364	0.4259840 +/- 0.0001	-2.01
	0.20	0.0237685679	0.0237573 +/- 0.0005	-0.95
	0.40	0.0630209469	0.0630315 +/- 0.0003	0.56
	0.60	0.0197690310	0.0197553 +/- 0.0006	-1.16
	0.80	0.0499450801	0.0499575 +/- 0.0003	0.83
	1.00	0.0028098955	0.0028133 +/- 0.0013	0.94
	1.20	0.0130114830	0.0130099 +/- 0.0007	-0.17
	1.40	0.0021885293	0.0021914 +/- 0.0015	0.88
	1.60	0.1094651813	0.1095050 +/- 0.0002	1.82
	2.00	0.0303790151	0.0304021 +/- 0.0004	1.90
	2.20	0.0125587643	0.0125614 +/- 0.0007	0.30
	2.40	0.0342983395	0.0343202 +/- 0.0004	1.59
	2.60	0.0050029697	0.0050019 +/- 0.001	-0.21
	2.80	0.0120878717	0.0120770 +/- 0.0006	-1.50
	3.00	0.0028725969	0.0028737 +/- 0.0012	0.32
	3.20	0.0574927055	0.0575015 +/- 0.0002	0.76
	total	0.8647406141	0.8647420 +/- 0.0000	0.00

Results: Weight-Windows

Tables 23 through 26 compare MCNP 5.1.50 calculated results using cell-based weight windows. The cell-based weight-windows used were generated by dividing each cylinder axially into ten smaller cylinders and use MCNP's weight-window generator. The source weight was changed from the default value of one to ten as an additional test of the lower weight-bounds being correctly generated. Therefore the results given are a factor of ten higher than the analytic answer.

TABLE 23: Weight-Windows MCNP Total Photon Leakage Current

Location	Analytic	MCNP 5 (R.E.)	Number of S.D away
Axis			
Region 1	0.889943	8.89943 +/- 0.0000	0.00
Region 2	0.764351	7.64372 +/- 0.0000	0.00
Diameter			
Region 1	0.254239	2.54234 +/- 0.0001	-0.20
Region 2	0.142818	1.42818 +/- 0.0001	0.00

TABLE 24: Weight-Windows MCNP Photon Surface Flux Results

Location	Energy (MeV)	Analytic	MCNP 5 (R.E.)	Number of S.D away
Axis				
Region 1	0.20	0.0431240772	0.431224 +/- 0.0002	-0.19
	0.40	0.0243696716	0.243716 +/- 0.0002	0.40
	0.80	0.1219679960	1.219580 +/- 0.0001	-0.82
	1.60	0.0688836141	0.688902 +/- 0.0001	0.96
	3.20	0.3312601617	3.312630 +/- 0.0000	0.00
Region 2				
	0.20	0.0930220670	0.930345 +/- 0.0001	1.34
	0.40	0.0497322033	0.497436 +/- 0.0002	1.15
	0.80	0.1291299684	1.291110 +/- 0.0001	-1.47
	1.60	0.0688836141	0.688931 +/- 0.0001	1.38
	3.20	0.1656300809	1.656300 +/- 0.0001	0.00

TABLE 25: Weight-Windows MCNP Photon Volume Flux Results

Location	Energy (MeV)	Analytic	MCNP 5 (R.E.)	Number of S.D away
Region 1	0.20	0.0552739100	0.552759 +/- 0.0002	0.18
	0.40	0.0316929622	0.316931 +/- 0.0002	0.02
	0.80	0.1956661722	1.956520 +/- 0.0001	-0.72
	1.60	0.0439941693	0.440044 +/- 0.0001	2.32
	3.20	0.4779073926	4.779000 +/- 0.0000	0.00
Region 2				
	0.20	0.0905357642	0.905414 +/- 0.0001	0.62
	0.40	0.0618684956	0.618722 +/- 0.0001	0.60
	0.80	0.1903885628	1.903690 +/- 0.0001	-1.03
	1.60	0.0716861089	0.716962 +/- 0.0001	1.41
	3.20	0.2389536963	2.389560 +/- 0.0001	0.10

TABLE 26: Weight-Windows MCNP Photon Pulse-Height Results

Location	Energy (MeV)	Analytic	MCNP 5 (R.E.)	Number of S.D away
Region 1	total	1.125288	11.2528 +/- 0.0000	0.00
Region 2	total	0.688563	6.88576 +/- 0.0001	0.19
Region 1	0.00	0.5000000000	5.0000400 +/- 0.0000	0.00
	1.60	0.1906154747	1.9061700 +/- 0.0001	0.08
	2.00	0.0607580302	0.6076300 +/- 0.0002	0.41
	2.20	0.0251175286	0.2511660 +/- 0.0003	-0.12
	2.40	0.0685966790	0.6858570 +/- 0.0002	-0.80
	2.60	0.0100059394	0.1000290 +/- 0.0004	-0.76
	2.80	0.0241757434	0.2418090 +/- 0.0003	0.71
	3.00	0.0057451938	0.0574901 +/- 0.0006	1.11
	3.20	0.1149854109	1.1498100 +/- 0.0001	-0.38
	total	1.0000000000	10.000000 +/- 0.0000	0.00
Region 2	0.00	0.4260696364	4.2606800 +/- 0.0001	-0.04
	0.20	0.0237685679	0.2375810 +/- 0.0003	-1.47
	0.40	0.0630209469	0.6303900 +/- 0.0002	1.43
	0.60	0.0197690310	0.1976390 +/- 0.0003	-0.87
	0.80	0.0499450801	0.4993410 +/- 0.0002	-1.10
	1.00	0.0028098955	0.0280921 +/- 0.0008	-0.31
	1.20	0.0130114830	0.1301410 +/- 0.0004	0.50
	1.40	0.0021885293	0.0219365 +/- 0.001	2.33
	1.60	0.1094651813	1.0946500 +/- 0.0001	-0.02
	2.00	0.0303790151	0.3037600 +/- 0.0003	-0.33
	2.20	0.0125587643	0.1255790 +/- 0.0004	-0.17
	2.40	0.0342983395	0.3429960 +/- 0.0002	0.18
	2.60	0.0050029697	0.0500489 +/- 0.0006	0.64
	2.80	0.0120878717	0.1208410 +/- 0.0004	-0.78
	3.00	0.0028725969	0.0287623 +/- 0.0008	1.58
	3.20	0.0574927055	0.5749570 +/- 0.0002	0.26
	total	0.8647406141	8.6474000 +/- 0.0000	0.00

Results: Weight-Windows and Forced Collisions

Tables 27 through 30 compare MCNP 5.1.50 calculated results using cell-based weight windows with forced collisions. As done previously, the cell-based weight-windows used were generated by dividing each cylinder into ten smaller cylinders and use MCNP's weight-window generator. Additionally, forced collisions was turned on in each of the ten smaller cylinders in both regions. The source weight was changed from the default value of one to ten as an additional test of the lower weight-bounds being correctly generated. The results given are thus a factor of ten higher than the analytic answer.

TABLE 27: Weight-Windows and Forced Collisions MCNP Total Photon Leakage Current

Location	Analytic	MCNP 5 (R.E.)	Number of S.D away
Axis			
Region 1	0.889943	8.89978 +/- 0.0000	0.00
Region 2	0.764351	7.64362 +/- 0.0000	0.00
Diameter			
Region 1	0.254239	2.54242 +/- 0.0001	0.12
Region 2	0.142818	1.42812 +/- 0.0001	-0.42

TABLE 28: Weight-Windows and Forced Collisions MCNP Photon Surface Flux Results

Location	Energy (MeV)	Analytic	MCNP 5 (R.E.)	Number of S.D away
Axis				
Region 1	0.20	0.0431240772	0.431300 +/- 0.0001	1.37
	0.40	0.0243696716	0.243745 +/- 0.0001	1.98
	0.80	0.1219679960	1.219820 +/- 0.0000	0.00
	1.60	0.0688836141	0.688813 +/- 0.0001	-0.34
	3.20	0.3312601617	3.312600 +/- 0.0000	0.00
Region 2				
	0.20	0.0930220670	0.930326 +/- 0.0001	1.13
	0.40	0.0497322033	0.497352 +/- 0.0001	0.60
	0.80	0.1291299684	1.291310 +/- 0.0001	0.08
	1.60	0.0688836141	0.688763 +/- 0.0001	-1.06
	3.20	0.1656300809	1.656300 +/- 0.0000	0.00

TABLE 29: Weight-Windows and Forced Collisions MCNP Photon Volume Flux Results

Location	Energy (MeV)	Analytic	MCNP 5 (R.E.)	Number of S.D away
Region 1	0.20	0.0552739100	0.552790 +/- 0.0001	0.92
	0.40	0.0316929622	0.316946 +/- 0.0001	0.52
	0.80	0.1956661722	1.956860 +/- 0.0000	0.00
	1.60	0.0439941693	0.439937 +/- 0.0001	-0.11
	3.20	0.4779073926	4.779070 +/- 0.0000	0.00
Region 2				
	0.20	0.0905357642	0.905396 +/- 0.0001	0.42
	0.40	0.0618684956	0.618697 +/- 0.0001	0.19
	0.80	0.1903885628	1.903900 +/- 0.0000	0.00
	1.60	0.0716861089	0.716791 +/- 0.0001	-0.98
	3.20	0.2389536963	2.389540 +/- 0.0000	0.00

TABLE 30: Weight-Windows and Forced Collisions MCNP Photon Pulse-Height Results

Location	Energy (MeV)	Analytic	MCNP 5 (R.E.)	Number of S.D away
Region 1	total	1.125288	11.2599 +/- 0.0008	0.78
Region 2	total	0.688563	6.89030 +/- 0.0008	0.85
Region 1	0.00	0.5000000000	5.0006800 +/- 0.0004	0.34
	1.60	0.1906154747	1.9066100 +/- 0.0003	0.80
	2.00	0.0607580302	0.6076980 +/- 0.0014	0.14
	2.20	0.0251175286	0.2525180 +/- 0.0042	1.27
	2.40	0.0685966790	0.6876510 +/- 0.0019	1.29
	2.60	0.0100059394	0.1012250 +/- 0.0128	0.90
	2.80	0.0241757434	0.2415170 +/- 0.0045	-0.22
	3.00	0.0057451938	0.0567637 +/- 0.0087	-1.39
	3.20	0.1149854109	1.1494600 +/- 0.0001	-3.43
	total	1.0000000000	10.004100 +/- 0.0004	
Region 2	0.00	0.4260696364	4.2602900 +/- 0.0002	-0.48
	0.20	0.0237685679	0.2383660 +/- 0.0057	0.50
	0.40	0.0630209469	0.6317750 +/- 0.0022	1.13
	0.60	0.0197690310	0.1990810 +/- 0.0058	1.20
	0.80	0.0499450801	0.4998820 +/- 0.0015	0.58
	1.00	0.0028098955	0.0281041 +/- 0.0013	0.14
	1.20	0.0130114830	0.1301540 +/- 0.0012	0.25
	1.40	0.0021885293	0.0219449 +/- 0.003	0.91
	1.60	0.1094651813	1.0948100 +/- 0.0002	0.72
	2.00	0.0303790151	0.3037580 +/- 0.0007	-0.15
	2.20	0.0125587643	0.1251730 +/- 0.0025	-1.33
	2.40	0.0342983395	0.3429210 +/- 0.0015	-0.12
	2.60	0.0050029697	0.0503897 +/- 0.0097	0.74
	2.80	0.0120878717	0.1217150 +/- 0.0067	1.03
	3.00	0.0028725969	0.0288769 +/- 0.019	0.28
	3.20	0.0574927055	0.5748450 +/- 0.0005	-0.29
	total	0.8647406141	8.6520900 +/- 0.0005	

Results: Weight-Windows with Exponential Transform

Tables 31 through 34 compare MCNP 5.1.50 calculated results using cell-based weight windows with exponential transform. As done previously, the cell-based weight-windows used were generated by axially dividing each cylinder into ten smaller cylinders and use MCNP's weight-window generator. Additionally, an exponential transform with a biasing parameter of -0.6 away from the source was turned on in each of the ten smaller cylinders in both regions. The source weight was changed from the default value of one to ten as an additional test of the lower weight-bounds being correctly generated. Therefore the results given are a factor of ten higher than the analytic answer.

TABLE 31: Weight-Windows with Exponential Transform MCNP Total Photon Leakage Current

Location	Analytic	MCNP 5 (R.E.)	Number of S.D away
Axis			
Region 1	0.889943	8.89954 +/- 0.0000	0.00
Region 2	0.764351	7.64360 +/- 0.0000	0.00
Diameter			
Region 1	0.254239	2.54250 +/- 0.0001	0.43
Region 2	0.142818	1.42819 +/- 0.0001	0.07

TABLE 32: Weight-Windows with Exponential Transform MCNP Photon Surface Flux Results

Location	Energy (MeV)	Analytic	MCNP 5 (R.E.)	Number of S.D away
Axis				
Region 1	0.20	0.0431240772	0.431224 +/- 0.0004	-0.10
	0.40	0.0243696716	0.243544 +/- 0.0003	-2.09
	0.80	0.1219679960	1.219860 +/- 0.0001	1.48
	1.60	0.0688836141	0.689066 +/- 0.0002	1.67
	3.20	0.3312601617	3.312440 +/- 0.0000	0.00
Region 2				
	0.20	0.0930220670	0.930153 +/- 0.0002	-0.36
	0.40	0.0497322033	0.497289 +/- 0.0002	-0.33
	0.80	0.1291299684	1.291450 +/- 0.0001	1.16
	1.60	0.0688836141	0.688934 +/- 0.0001	1.42
	3.20	0.1656300809	1.656220 +/- 0.0000	0.00

TABLE 33: Weight-Windows with Exponential Transform MCNP Photon Volume Flux Results

Location	Energy (MeV)	Analytic	MCNP 5 (R.E.)	Number of S.D away
Region 1	0.20	0.0552739100	0.552756 +/- 0.0002	0.15
	0.40	0.0316929622	0.316937 +/- 0.0003	0.08
	0.80	0.1956661722	1.956590 +/- 0.0001	-0.37
	1.60	0.0439941693	0.440089 +/- 0.0002	1.67
	3.20	0.4779073926	4.779020 +/- 0.0000	0.00
Region 2				
	0.20	0.0905357642	0.905386 +/- 0.0002	0.16
	0.40	0.0618684956	0.618639 +/- 0.0002	-0.37
	0.80	0.1903885628	1.903950 +/- 0.0001	0.34
	1.60	0.0716861089	0.717015 +/- 0.0001	2.15
	3.20	0.2389536963	2.389440 +/- 0.0000	0.00

TABLE 34: Weight-Windows with Exponential Transform MCNP Photon Pulse-Height Results

Location	Energy (MeV)	Analytic	MCNP 5 (R.E.)	Number of S.D away
Region 1	total	1.125288	11.2530 +/- 0.0001	0.11
Region 2	total	0.688563	6.88539 +/- 0.0001	-0.35
Region 1	0.00	0.5000000000	4.9997500 +/- 0.0000	0.00
	1.60	0.1906154747	1.9065500 +/- 0.0001	2.07
	2.00	0.0607580302	0.6075330 +/- 0.0002	-0.39
	2.20	0.0251175286	0.2512600 +/- 0.0003	1.12
	2.40	0.0685966790	0.6857870 +/- 0.0002	-1.31
	2.60	0.0100059394	0.1000020 +/- 0.0006	-0.96
	2.80	0.0241757434	0.2416260 +/- 0.0004	-1.36
	3.00	0.0057451938	0.0573814 +/- 0.0008	-1.54
	3.20	0.1149854109	1.1500400 +/- 0.0002	0.81
	total	1.0000000000	9.9999400 +/- 0.0000	0.00
Region 2	0.00	0.4260696364	4.2608600 +/- 0	0.00
	0.20	0.0237685679	0.2376570 +/- 0.0004	-0.30
	0.40	0.0630209469	0.6299280 +/- 0.0002	-2.23
	0.60	0.0197690310	0.1976290 +/- 0.0004	-0.78
	0.80	0.0499450801	0.4996980 +/- 0.0003	1.65
	1.00	0.0028098955	0.0280943 +/- 0.0008	-0.21
	1.20	0.0130114830	0.1301540 +/- 0.0005	0.60
	1.40	0.0021885293	0.0219209 +/- 0.0012	1.35
	1.60	0.1094651813	1.0944800 +/- 0.0001	-1.57
	2.00	0.0303790151	0.3038260 +/- 0.0002	0.59
	2.20	0.0125587643	0.1256150 +/- 0.0004	0.54
	2.40	0.0342983395	0.3429600 +/- 0.0002	-0.34
	2.60	0.0050029697	0.0499806 +/- 0.0006	-1.64
	2.80	0.0120878717	0.1208090 +/- 0.0004	-1.44
	3.00	0.0028725969	0.0287625 +/- 0.0009	1.41
	3.20	0.0574927055	0.5749360 +/- 0.0002	0.08
	total	0.8647406141	8.6473100 +/- 0.0000	0.00

Comparison of Analytic Solution with MCNP 5.1.50 Calculated Results for Coupled Photon-Electron Transport with Variance Reduction

MCNP can calculate pulse-heights when the source particle or progeny is a photon or electron and if both photons and electrons are being transported. Most MCNP users who calculate pulse-heights usually require coupled photon and electron transport. However, the collision physics in figure 1 does not include electrons as progeny and therefore, there is no analytic solution to compare with. However, the energy deposited in each collision can be treated as generating a real electron with that energy. This electron and all of its progeny (e.g. electrons, bremsstraluung photons, x-rays, Auger electrons, etc) are transported in an infinite detector cell using real arbitrary atomic data. The infinite detector cell is modeled by making all boundaries reflecting for those particles. Therefore none of these particles escapes and the pulse-height tally is preserved. Treating the deposited energy as an electron-photon cascade produces much longer and complicated history trees that further test the new variance reduction algorithm by creating some of the physical photon and electron creation and termination mechanisms that would not have ordinarily been tested a photon only problem (e.g. bremsstrahluung photons, x-rays, photo-electrons, Compton electrons, knock-on electrons, Auger electrons). The electron energy cutoff was the default value of 1 keV. The addition of the photon-electron cascade inside the infinite detector stresses the history tree and not the variance reduction since these particles are not allowed to leak and will not contribute to any tally.

As before, all MCNP calculated results match the analytic solutions to four or five significant figures and are normally distributed. Similarly, there are a few results with relative errors of zero or standard deviations greater than two. The 'number of SD away' values are considered to be unreliable since the relative error is printed out to only five decimal places.

Results: Analog MCNP Results for Coupled Photon/Electron Transport

Tables 35 through 37 compare analytic results with MCNP 5.1.50 results run in analog mode. This would be considered the 'default' case and is identical to the results generated forcing the use of the 'tree' structure used to track the various variance reduction branches. The

TABLE 35: Analog MCNP Total Photon Leakage Current

Location	Analytic	MCNP 5 (R.E.)	Number of S.D away
Axis			
Region 1	0.889943	0.890177 +/- 0.0001	2.63
Region 2	0.764351	0.764511 +/- 0.0002	1.05
Diameter			
Region 1	0.254239	0.254165 +/- 0.0006	-0.49
Region 2	0.142818	0.142944 +/- 0.0009	0.98

TABLE 36: Analog MCNP Photon Surface Flux Results

Location	Energy (MeV)	Analytic	MCNP 5 (R.E.)	Number of S.D away
Axis				
Region 1	0.20	0.0431240772	0.0431055 +/- 0.0016	-0.27
	0.40	0.0243696716	0.0243435 +/- 0.0016	-0.67
	0.80	0.1219679960	0.1218870 +/- 0.0007	-0.95
	1.60	0.0688836141	0.0690698 +/- 0.0009	3.00
	3.20	0.3312601617	0.3313540 +/- 0.0003	0.94
Region 2				
	0.20	0.0930220670	0.0929208 +/- 0.001	-1.09
	0.40	0.0497322033	0.0497567 +/- 0.0011	0.45
	0.80	0.1291299684	0.1292280 +/- 0.0006	1.26
	1.60	0.0688836141	0.0689128 +/- 0.0009	0.47
	3.20	0.1656300809	0.1656860 +/- 0.0005	0.68
Diameter				
Region 1	0.20	0.0303893949	0.0303979 +/- 0.0013	0.22
	0.40	0.0124222561	0.0124146 +/- 0.0016	-0.39
	0.80	0.0414075202	0.0413821 +/- 0.0008	-0.77
Region 2	0.20	0.0160899440	0.0160898 +/- 0.0018	0.00
	0.40	0.0105163539	0.0105433 +/- 0.0017	1.50
	0.80	0.0207037601	0.0207186 +/- 0.0012	0.60

TABLE 37: Analog MCNP Photon Pulse-Height Results

Location	Energy (MeV)	Analytic	MCNP 5 (R.E.)	Number of S.D away
Region 1	total	1.125288	1.124570 +/- 0.0003	-2.13
Region 2	total	0.688563	0.688837 +/- 0.0005	0.80
Region 1	0.00	0.5000000000	0.5001420 +/- 0.0003	0.95
	1.60	0.1906154747	0.1908020 +/- 0.0007	1.40
	2.00	0.0607580302	0.0608153 +/- 0.0012	0.78
	2.20	0.0251175286	0.0251221 +/- 0.002	0.09
	2.40	0.0685966790	0.0685187 +/- 0.0012	-0.95
	2.60	0.0100059394	0.0099869 +/- 0.0031	-0.61
	2.80	0.0241757434	0.0241125 +/- 0.002	-1.31
	3.00	0.0057451938	0.0057073 +/- 0.0042	-1.58
	3.20	0.1149854109	0.1147930 +/- 0.0009	-1.86
	total	1.0000000000	1.0000000 +/- 0.0000	
Region 2	0.00	0.4260696364	0.4260740 +/- 0.0004	0.03
	0.20	0.0237685679	0.0237754 +/- 0.002	0.14
	0.40	0.0630209469	0.0630173 +/- 0.0012	-0.05
	0.60	0.0197690310	0.0196798 +/- 0.0022	-2.06
	0.80	0.0499450801	0.0500267 +/- 0.0014	1.17
	1.00	0.0028098955	0.0028265 +/- 0.0059	1.00
	1.20	0.0130114830	0.0130714 +/- 0.0027	1.70
	1.40	0.0021885293	0.0022040 +/- 0.0067	1.05
	1.60	0.1094651813	0.1096690 +/- 0.0009	2.06
	2.00	0.0303790151	0.0303492 +/- 0.0018	-0.55
	2.20	0.0125587643	0.0125636 +/- 0.0028	0.14
	2.40	0.0342983395	0.0343137 +/- 0.0017	0.26
	2.60	0.0050029697	0.0050024 +/- 0.0045	-0.03
	2.80	0.0120878717	0.0120436 +/- 0.0029	-1.27
	3.00	0.0028725969	0.0028625 +/- 0.0059	-0.60
	3.20	0.0574927055	0.0574907 +/- 0.0013	-0.03
	total	0.8647406141	0.8649690 +/- 0.0001	

Results: Geometry Splitting and Russian Roulette

Tables 38 through 40 compare MCNP 5.1.50 calculated results using non-integer geometry splitting with Russian Roulette turned **on**. A new variance reduction option was added for pulse-height tallies to turn off Russian Roulette to avoid removing substantial portions of the history tree if a particle does not survive the roulette. Tables 41 through 43 compare MCNP 5.1.50 calculated results using non-integer geometry splitting with Russian Roulette turned **off**. The two cylinders were sub-divided into 10 smaller cylinders each. Each of these new cells' importances were specified such that the ratio of neighboring cell importances was not an integer value. Additionally, the importances increased and decreased across the cylinder's axis to stress the geometry splitting and Russian Roulette capabilities.

TABLE 38: Geometry Splitting/Russian Roulette MCNP Total Photon Leakage Current

Location	Analytic	MCNP 5 (R.E.)	Number of S.D away
Axis			
Region 1	0.889943	0.890066 +/- 0.0003	0.46
Region 2	0.764351	0.764331 +/- 0.0004	-0.07
Diameter			
Region 1	0.254239	0.254118 +/- 0.0004	-1.19
Region 2	0.142818	0.142836 +/- 0.0002	0.63

TABLE 39: Geometry Splitting/Russian Roulette MCNP Photon Surface Flux Results

Location	Energy (MeV)	Analytic	MCNP 5 (R.E.)	Number of S.D away
Axis				
Region 1	0.20	0.0431240772	0.0430785 +/- 0.0015	-0.71
	0.40	0.0243696716	0.0244166 +/- 0.0016	1.20
	0.80	0.1219679960	0.1218410 +/- 0.0007	-1.49
	1.60	0.0688836141	0.0689165 +/- 0.001	0.48
	3.20	0.3312601617	0.3314340 +/- 0.0005	1.05
Region 2				
	0.20	0.0930220670	0.0929832 +/- 0.0007	-0.60
	0.40	0.0497322033	0.0497276 +/- 0.0007	-0.13
	0.80	0.1291299684	0.1290630 +/- 0.0005	-1.04
	1.60	0.0688836141	0.0688799 +/- 0.0007	-0.08
	3.20	0.1656300809	0.1657310 +/- 0.0005	1.22
Diameter				
Region 1	0.20	0.0303893949	0.0303592 +/- 0.001	-1.00
	0.40	0.0124222561	0.0124238 +/- 0.0012	0.11
	0.80	0.0414075202	0.0414135 +/- 0.0006	0.24
Region 2	0.20	0.0160899440	0.0161028 +/- 0.0009	0.88
	0.40	0.0105163539	0.0105095 +/- 0.0009	-0.73
	0.80	0.0207037601	0.0207130 +/- 0.0007	0.64

TABLE 40: Geometry Splitting/Russian Roulette MCNP Photon Pulse-Height Results

Location	Energy (MeV)	Analytic	MCNP 5 (R.E.)	Number of S.D away
Region 1	total	1.125288	1.12457 +/- 0.0005	-1.28
Region 2	total	0.688563	0.68889 +/- 0.0004	1.19
Region 1	0.00	0.5000000000	0.5002940 +/- 0.0005	1.18
	1.60	0.1906154747	0.1906000 +/- 0.0008	-0.10
	2.00	0.0607580302	0.0606034 +/- 0.0016	-1.59
	2.20	0.0251175286	0.0250327 +/- 0.0024	-1.41
	2.40	0.0685966790	0.0686079 +/- 0.0013	0.13
	2.60	0.0100059394	0.0099333 +/- 0.0042	-1.74
	2.80	0.0241757434	0.0242185 +/- 0.0024	0.74
	3.00	0.0057451938	0.0057229 +/- 0.0049	-0.79
	3.20	0.1149854109	0.1149560 +/- 0.0007	-0.37
	total	1.0000000000	0.9999690 +/- 0.0003	
Region 2	0.00	0.4260696364	0.4260380 +/- 0.0004	-0.19
	0.20	0.0237685679	0.0237355 +/- 0.0022	-0.63
	0.40	0.0630209469	0.0629943 +/- 0.0009	-0.47
	0.60	0.0197690310	0.0197595 +/- 0.0012	-0.40
	0.80	0.0499450801	0.0499101 +/- 0.0008	-0.88
	1.00	0.0028098955	0.0028060 +/- 0.0026	-0.53
	1.20	0.0130114830	0.0130224 +/- 0.0015	0.56
	1.40	0.0021885293	0.0021964 +/- 0.0029	1.24
	1.60	0.1094651813	0.1095100 +/- 0.0006	0.68
	2.00	0.0303790151	0.0303696 +/- 0.0009	-0.34
	2.20	0.0125587643	0.0125417 +/- 0.0013	-1.05
	2.40	0.0342983395	0.0343360 +/- 0.0008	1.37
	2.60	0.0050029697	0.0050167 +/- 0.0018	1.52
	2.80	0.0120878717	0.0120904 +/- 0.0012	0.17
	3.00	0.0028725969	0.0028703 +/- 0.0024	-0.33
	3.20	0.0574927055	0.0575600 +/- 0.0007	1.67
	total	0.8647406141	0.8647580 +/- 0.0004	

TABLE 41: Geometry Splitting MCNP Total Photon Leakage Current

Location	Analytic	MCNP 5 (R.E.)	Number of S.D away
Axis			
Region 1	0.889943	0.889969 +/- 0.0001	0.29
Region 2	0.764351	0.764336 +/- 0.0001	-0.20
Diameter			
Region 1	0.254239	0.254118 +/- 0.0004	-1.19
Region 2	0.142818	0.142836 +/- 0.0002	0.63

TABLE 42: Geometry Splitting MCNP Photon Surface Flux Results

Location	Energy (MeV)	Analytic	MCNP 5 (R.E.)	Number of S.D away
Axis				
Region 1	0.20	0.0431240772	0.0431443 +/- 0.0007	0.67
	0.40	0.0243696716	0.0243544 +/- 0.0007	-0.90
	0.80	0.1219679960	0.1219520 +/- 0.0003	-0.44
	1.60	0.0688836141	0.0689193 +/- 0.0005	1.04
	3.20	0.3312601617	0.3312520 +/- 0.0002	-0.12
Region 2				
	0.20	0.0930220670	0.0930236 +/- 0.0003	0.05
	0.40	0.0497322033	0.0497303 +/- 0.0003	-0.13
	0.80	0.1291299684	0.1291210 +/- 0.0002	-0.35
	1.60	0.0688836141	0.0688882 +/- 0.0003	0.22
	3.20	0.1656300809	0.1656250 +/- 0.0002	-0.15
Diameter				
Region 1	0.20	0.0303893949	0.0303515 +/- 0.0008	-1.56
	0.40	0.0124222561	0.0124024 +/- 0.0009	-1.78
	0.80	0.0414075202	0.0414255 +/- 0.0005	0.87
Region 2	0.20	0.0160899440	0.0160941 +/- 0.0003	0.86
	0.40	0.0105163539	0.0105188 +/- 0.0003	0.78
	0.80	0.0207037601	0.0207032 +/- 0.0003	-0.09

TABLE 43: Geometry Splitting MCNP Photon Pulse-Height Results

Location	Energy (MeV)	Analytic	MCNP 5 (R.E.)	Number of S.D away
Region 1	total	1.125288	1.124990 +/- 0.0002	-1.32
Region 2	total	0.688563	0.688512 +/- 0.0002	-0.37
Region 1	0.00	0.5000000000	0.4999620 +/- 0.0002	-0.38
	1.60	0.1906154747	0.1906860 +/- 0.0003	1.23
	2.00	0.0607580302	0.0607159 +/- 0.0006	-1.16
	2.20	0.0251175286	0.0251123 +/- 0.001	-0.21
	2.40	0.0685966790	0.0685960 +/- 0.0006	-0.02
	2.60	0.0100059394	0.0099805 +/- 0.0014	-1.82
	2.80	0.0241757434	0.0241611 +/- 0.0009	-0.67
	3.00	0.0057451938	0.0057332 +/- 0.0019	-1.10
	3.20	0.1149854109	0.1149340 +/- 0.0005	-0.89
	total	1.0000000000	0.9998810 +/- 0.0001	
Region 2	0.00	0.4260696364	0.4260700 +/- 0.0001	0.01
	0.20	0.0237685679	0.0237663 +/- 0.0007	-0.14
	0.40	0.0630209469	0.0630106 +/- 0.0003	-0.55
	0.60	0.0197690310	0.0197598 +/- 0.0004	-1.17
	0.80	0.0499450801	0.0499542 +/- 0.0003	0.61
	1.00	0.0028098955	0.0028097 +/- 0.0009	-0.08
	1.20	0.0130114830	0.0130155 +/- 0.0006	0.51
	1.40	0.0021885293	0.0021887 +/- 0.001	0.06
	1.60	0.1094651813	0.1094540 +/- 0.0002	-0.51
	2.00	0.0303790151	0.0303787 +/- 0.0003	-0.03
	2.20	0.0125587643	0.0125681 +/- 0.0004	1.86
	2.40	0.0342983395	0.0342856 +/- 0.0003	-1.24
	2.60	0.0050029697	0.0050082 +/- 0.0006	1.75
	2.80	0.0120878717	0.0120828 +/- 0.0004	-1.05
	3.00	0.0028725969	0.0028705 +/- 0.0008	-0.91
	3.20	0.0574927055	0.0574873 +/- 0.0003	-0.31
	total	0.8647406141	0.8647100 +/- 0.0001	

Results: Implicit Capture and Weight Cutoff

Tables 44 through 46 compare MCNP 5.1.50 calculated results using the default implicit capture and weight cutoff variance reduction techniques.

TABLE 44: Impl. Capt./Wgt. Cut MCNP Total Photon Leakage Current

Location	Analytic	MCNP 5 (R.E.)	Number of S.D away
Axis			
Region 1	0.889943	0.889969 +/- 0.0001	0.29
Region 2	0.764351	0.764511 +/- 0.0002	1.05
Diameter			
Region 1	0.254239	0.254165 +/- 0.0006	-0.49
Region 2	0.142818	0.142944 +/- 0.0009	0.98

TABLE 45: Impl. Capt./Wgt. Cut MCNP Photon Surface Flux Results

Location	Energy (MeV)	Analytic	MCNP 5 (R.E.)	Number of S.D away
Axis				
Region 1	0.20	0.0431240772	0.0431443 +/- 0.0007	0.67
	0.40	0.0243696716	0.0243544 +/- 0.0007	-0.90
	0.80	0.1219679960	0.1219520 +/- 0.0003	-0.44
	1.60	0.0688836141	0.0689193 +/- 0.0005	1.04
	3.20	0.3312601617	0.3312520 +/- 0.0002	-0.12
Region 2				
	0.20	0.0930220670	0.0929208 +/- 0.001	-1.09
	0.40	0.0497322033	0.0497567 +/- 0.0011	0.45
	0.80	0.1291299684	0.1292280 +/- 0.0006	1.26
	1.60	0.0688836141	0.0689128 +/- 0.0009	0.47
	3.20	0.1656300809	0.1656860 +/- 0.0005	0.68
Diameter				
Region 1	0.20	0.0303893949	0.0303979 +/- 0.0013	0.22
	0.40	0.0124222561	0.0124146 +/- 0.0016	-0.39
	0.80	0.0414075202	0.0413821 +/- 0.0008	-0.77
Region 2	0.20	0.0160899440	0.0160898 +/- 0.0018	0.00
	0.40	0.0105163539	0.0105433 +/- 0.0017	1.50
	0.80	0.0207037601	0.0207186 +/- 0.0012	0.60

TABLE 46: Impl. Capt./Wgt. Cut MCNP Photon Pulse-Height Results

Location	Energy (MeV)	Analytic	MCNP 5 (R.E.)	Number of S.D away
Region 1	total	1.125288	1.124570 +/- 0.000	-2.13
Region 2	total	0.688563	0.688512 +/- 0.000	-0.37
Region 1	0.00	0.5000000000	0.5001420 +/- 0.000	0.95
	1.60	0.1906154747	0.1908020 +/- 0.000	1.40
	2.00	0.0607580302	0.0608153 +/- 0.001	0.78
	2.20	0.0251175286	0.0251221 +/- 0.002	0.09
	2.40	0.0685966790	0.0685187 +/- 0.001	-0.95
	2.60	0.0100059394	0.0099869 +/- 0.003	-0.61
	2.80	0.0241757434	0.0241125 +/- 0.002	-1.31
	3.00	0.0057451938	0.0057073 +/- 0.004	-1.58
	3.20	0.1149854109	0.1147930 +/- 0.000	-1.86
	total	1.0000000000	1.0000000 +/- 0.000	0.00
Region 2	0.00	0.4260696364	0.4260740 +/- 0.000	0.03
	0.20	0.0237685679	0.0237754 +/- 0.002	0.14
	0.40	0.0630209469	0.0630173 +/- 0.001	-0.05
	0.60	0.0197690310	0.0196798 +/- 0.002	-2.06
	0.80	0.0499450801	0.0500267 +/- 0.001	1.17
	1.00	0.0028098955	0.0028265 +/- 0.005	1.00
	1.20	0.0130114830	0.0130714 +/- 0.002	1.70
	1.40	0.0021885293	0.0022040 +/- 0.006	1.05
	1.60	0.1094651813	0.1096690 +/- 0.000	2.06
	2.00	0.0303790151	0.0303492 +/- 0.001	-0.55
	2.20	0.0125587643	0.0125636 +/- 0.002	0.14
	2.40	0.0342983395	0.0343137 +/- 0.001	0.26
	2.60	0.0050029697	0.0050024 +/- 0.004	-0.03
	2.80	0.0120878717	0.0120436 +/- 0.002	-1.27
	3.00	0.0028725969	0.0028625 +/- 0.005	-0.60
	3.20	0.0574927055	0.0574907 +/- 0.001	-0.03
	total	0.8647406141	0.8649690 +/- 0.000	0.00

Results: Weight-Windows

Tables 47 through 49 compare MCNP 5.1.50 calculated results using cell-based weight windows. The cell-based weight-windows used were generated by dividing each cylinder into ten smaller cylinders and use MCNP's weight-window generator. The source weight was changed from the default value of one to ten as an additional test of the lower weight-bounds being correctly generated. Therefore the results given are a factor of ten higher than the analytic answer.

TABLE 47: Impl. Capt./Wgt. Cut MCNP Total Photon Leakage Current

Location	Analytic	MCNP 5 (R.E.)	Number of S.D away
<u>Axis</u>			
Region 1	0.889943	8.89901 +/- 0.0001	-0.47
Region 2	0.764351	7.64356 +/- 0.0001	0.07
<u>Diameter</u>			
Region 1	0.254239	2.54142 +/- 0.0003	-1.27
Region 2	0.142818	1.42816 +/- 0.0004	-0.04

TABLE 48: Weight-Windows MCNP Photon Surface Flux Results

Location	Energy (MeV)	Analytic	MCNP 5 (R.E.)	Number of S.D away
Axis				
Region 1	0.20	0.0431240772	0.4308760 +/- 0.0007	-1.21
	0.40	0.0243696716	0.2436050 +/- 0.0007	-0.54
	0.80	0.1219679960	1.2190900 +/- 0.0003	-1.61
	1.60	0.0688836141	0.6890260 +/- 0.0004	0.69
	3.20	0.3312601617	3.3131800 +/- 0.0001	1.75
Region 2				
	0.20	0.0930220670	0.9302280 +/- 0.0005	0.02
	0.40	0.0497322033	0.4971090 +/- 0.0005	-0.86
	0.80	0.1291299684	1.2906400 +/- 0.0003	-1.70
	1.60	0.0688836141	0.6892430 +/- 0.0004	1.48
	3.20	0.1656300809	1.6568000 +/- 0.0002	1.51
Diameter				
Region 1	0.20	0.0303893949	0.3037012 +/- 0.0006	-1.06
	0.40	0.0124222561	0.1240660 +/- 0.0007	-1.80
	0.80	0.0414075202	0.4141021 +/- 0.0004	0.16
Region 2	0.20	0.0160899440	0.1610602 +/- 0.0008	1.25
	0.40	0.0105163539	0.1050649 +/- 0.0008	-1.17
	0.80	0.0207037601	0.2069662 +/- 0.0005	-0.69

TABLE 49: Weight-Windows MCNP Photon Pulse-Height Results

Location	Energy (MeV)	Analytic	MCNP 5 (R.E.)	Number of S.D away
Region 1	total	1.125288	1.124570 +/- 0.000	-2.13
Region 2	total	0.688563	0.688512 +/- 0.000	-0.37
Region 1	0.00	0.5000000000	0.5001420 +/- 0.000	0.95
	1.60	0.1906154747	0.1908020 +/- 0.000	1.40
	2.00	0.0607580302	0.0608153 +/- 0.001	0.78
	2.20	0.0251175286	0.0251221 +/- 0.002	0.09
	2.40	0.0685966790	0.0685187 +/- 0.001	-0.95
	2.60	0.0100059394	0.0099869 +/- 0.003	-0.61
	2.80	0.0241757434	0.0241125 +/- 0.002	-1.31
	3.00	0.0057451938	0.0057073 +/- 0.004	-1.58
	3.20	0.1149854109	0.1147930 +/- 0.000	-1.86
	total	1.0000000000	1.0000000 +/- 0.000	0.00
Region 2	0.00	0.4260696364	0.4260740 +/- 0.000	0.03
	0.20	0.0237685679	0.0237754 +/- 0.002	0.14
	0.40	0.0630209469	0.0630173 +/- 0.001	-0.05
	0.60	0.0197690310	0.0196798 +/- 0.002	-2.06
	0.80	0.0499450801	0.0500267 +/- 0.001	1.17
	1.00	0.0028098955	0.0028265 +/- 0.005	1.00
	1.20	0.0130114830	0.0130714 +/- 0.002	1.70
	1.40	0.0021885293	0.0022040 +/- 0.006	1.05
	1.60	0.1094651813	0.1096690 +/- 0.000	2.06
	2.00	0.0303790151	0.0303492 +/- 0.001	-0.55
	2.20	0.0125587643	0.0125636 +/- 0.002	0.14
	2.40	0.0342983395	0.0343137 +/- 0.001	0.26
	2.60	0.0050029697	0.0050024 +/- 0.004	-0.03
	2.80	0.0120878717	0.0120436 +/- 0.002	-1.27
	3.00	0.0028725969	0.0028625 +/- 0.005	-0.60
	3.20	0.0574927055	0.0574907 +/- 0.001	-0.03
	total	0.8647406141	0.8649690 +/- 0.000	0.00

Results: Weight-Windows and Forced Collisions

Tables 50 through 52 compare MCNP 5.1.50 calculated results using cell-based weight windows with forced collisions. As done previously, the cell-based weight-windows used were generated by dividing each cylinder into ten smaller cylinders and use MCNP's weight-window generator. Additionally, forced collisions was turned on in each of the ten smaller cylinders in both regions. The source weight was changed from the default value of one to ten as an additional test of the lower weight-bounds being correctly generated. The results given are thus a factor of ten higher than the analytic answer.

TABLE 50: Weight-Windows/Forced-Collisions MCNP Total Photon Leakage Current

Location	Analytic	MCNP 5 (R.E.)	Number of S.D away
Axis			
Region 1	0.889943	8.89969 +/- 0.0001	0.29
Region 2	0.764351	7.64458 +/- 0.0001	1.40
Diameter			
Region 1	0.254239	2.54352 +/- 0.0003	1.48
Region 2	0.142818	1.42776 +/- 0.0002	-1.47

TABLE 51: Weight-Windows/Forced-Collisions MCNP Photon Surface Flux Results

Location	Energy (MeV)	Analytic	MCNP 5 (R.E.)	Number of S.D away
Axis				
Region 1	0.20	0.0431240772	0.431301 +/- 0.0003	0.47
	0.40	0.0243696716	0.243740 +/- 0.0004	0.44
	0.80	0.1219679960	1.219730 +/- 0.0002	0.21
	1.60	0.0688836141	0.688855 +/- 0.0002	0.14
	3.20	0.3312601617	3.312600 +/- 0	0.00
Region 2				
	0.20	0.0930220670	0.930490 +/- 0.0003	0.96
	0.40	0.0497322033	0.497396 +/- 0.0003	0.50
	0.80	0.1291299684	1.291390 +/- 0.0002	0.35
	1.60	0.0688836141	0.689108 +/- 0.0002	1.97
	3.20	0.1656300809	1.656300 +/- 0	0.00
Diameter				
Region 1	0.20	0.0303893949	0.304084 +/- 0.0003	2.08
	0.40	0.0124222561	0.124230 +/- 0.0004	0.15
	0.80	0.0414075202	0.414255 +/- 0.0002	2.17
Region 2	0.20	0.0160899440	0.160842 +/- 0.0003	-1.19
	0.40	0.0105163539	0.105137 +/- 0.0003	-0.84
	0.80	0.0207037601	0.206982 +/- 0.0002	-1.34

TABLE 52: Weight-Windows/Forced-Collisions MCNP Photon Pulse-Height Results

Location	Energy (MeV)	Analytic	MCNP 5 (R.E.)	Number of S.D away
Region 1	total	1.125288	11.2733 +/- 0.0031	0.58
Region 2	total	0.688563	6.91821 +/- 0.0033	1.43
Region 1	0.00	0.5000000000	5.0125200 +/- 0.0016	1.56
	1.60	0.1906154747	1.9047800 +/- 0.0009	-0.80
	2.00	0.0607580302	0.6071260 +/- 0.0044	-0.17
	2.20	0.0251175286	0.2476630 +/- 0.011	-1.29
	2.40	0.0685966790	0.6870380 +/- 0.005	0.31
	2.60	0.0100059394	0.1106900 +/- 0.0704	1.36
	2.80	0.0241757434	0.2427920 +/- 0.0127	0.34
	3.00	0.0057451938	0.0573352 +/- 0.0263	-0.08
	3.20	0.1149854109	1.1494000 +/- 0.0005	-0.79
	total	1.0000000000	10.019300 +/- 0.0016	
Region 2	0.00	0.4260696364	4.2643300 +/- 0.0007	1.22
	0.20	0.0237685679	0.2435040 +/- 0.0201	1.19
	0.40	0.0630209469	0.6389360 +/- 0.012	1.14
	0.60	0.0197690310	0.1915360 +/- 0.0154	-2.09
	0.80	0.0499450801	0.4964190 +/- 0.0033	-1.85
	1.00	0.0028098955	0.0280039 +/- 0.004	-0.85
	1.20	0.0130114830	0.1302950 +/- 0.0037	0.37
	1.40	0.0021885293	0.0220816 +/- 0.0094	0.95
	1.60	0.1094651813	1.0946500 +/- 0.0005	0.00
	2.00	0.0303790151	0.3039820 +/- 0.0021	0.30
	2.20	0.0125587643	0.1244790 +/- 0.0078	-1.14
	2.40	0.0342983395	0.3446350 +/- 0.0053	0.90
	2.60	0.0050029697	0.0526917 +/- 0.0331	1.53
	2.80	0.0120878717	0.1280050 +/- 0.0396	1.41
	3.00	0.0028725969	0.0299563 +/- 0.0352	1.17
	3.20	0.0574927055	0.5752940 +/- 0.0007	0.91
	total	0.8647406141	8.6688000 +/- 0.0018	

Results: Weight-Windows with Exponential Transform

Tables 53 through 55 compare MCNP 5.1.50 calculated results using cell-based weight windows with exponential transform. As done previously, the cell-based weight-windows used were generated by dividing each cylinder into ten smaller cylinders and use MCNP's weight-window generator. Additionally, an exponential transform with a biasing parameter of -0.6 away from the source was turned on in each of the ten smaller cylinders in both regions. The source weight was changed from the default value of one to ten as an additional test of the lower weight-bounds being correctly generated. Therefore the results given are a factor of ten higher than the analytic answer.

TABLE 53: Weight-Windows/Exponential Transform MCNP Total Photon Leakage Current

Location	Analytic	MCNP 5 (R.E.)	Number of S.D away
Axis			
Region 1	0.889943	8.89698 +/- 0.0001	-2.75
Region 2	0.764351	7.64117 +/- 0.0001	-3.06
Diameter			
Region 1	0.254239	2.54049 +/- 0.0004	-1.87
Region 2	0.142818	1.42797 +/- 0.0004	-0.37

TABLE 54: Weight-Windows/Exponential Transform MCNP Photon Surface Flux Results

Location	Energy (MeV)	Analytic	MCNP 5 (R.E.)	Number of S.D away
Axis				
Region 1	0.20	0.0431240772	0.4302820 +/- 0.0011	-2.03
	0.40	0.0243696716	0.2434030 +/- 0.0011	-1.10
	0.80	0.1219679960	1.2188300 +/- 0.0004	-1.74
	1.60	0.0688836141	0.6889920 +/- 0.0005	0.45
	3.20	0.3312601617	3.3129200 +/- 0.0001	0.00
Region 2				
	0.20	0.0930220670	0.9291670 +/- 0.0006	-1.89
	0.40	0.0497322033	0.4973380 +/- 0.0006	0.05
	0.80	0.1291299684	1.2905500 +/- 0.0003	-1.94
	1.60	0.0688836141	0.6887260 +/- 0.0004	-0.40
	3.20	0.1656300809	1.6566400 +/- 0.0001	0.00
Diameter				
Region 1	0.20	0.0303893949	0.3036939 +/- 0.0006	-1.10
	0.40	0.0124222561	0.1241044 +/- 0.0008	-1.19
	0.80	0.0414075202	0.4137642 +/- 0.0005	-1.50
Region 2	0.20	0.0160899440	0.1609210 +/- 0.0007	0.19
	0.40	0.0105163539	0.1052404 +/- 0.0008	0.91
	0.80	0.0207037601	0.2068675 +/- 0.0006	-1.37

TABLE 55: Weight-Windows/Exponential Transform MCNP Photon Pulse-Height Results

Location	Energy (MeV)	Analytic	MCNP 5 (R.E.)	Number of S.D away
Region 1		1.125288	11.248800 +/- 0.0003	-1.21
Region 2		0.688563	6.8846300 +/- 0.0004	-0.36
Region 1	0.00	0.5000000000	4.9999300 +/- 0.0001	-0.14
	1.60	0.1906154747	1.9060300 +/- 0.0004	-0.16
	2.00	0.0607580302	0.6070100 +/- 0.0007	-1.34
	2.20	0.0251175286	0.2508580 +/- 0.0011	-1.15
	2.40	0.0685966790	0.6856600 +/- 0.0007	-0.64
	2.60	0.0100059394	0.0998131 +/- 0.0018	-1.37
	2.80	0.0241757434	0.2415540 +/- 0.0012	-0.70
	3.00	0.0057451938	0.0573316 +/- 0.0026	-0.81
	3.20	0.1149854109	1.1499400 +/- 0.0006	0.12
	total	1.0000000000	9.9981200 +/- 0.0001	
Region 2	0.00	0.4260696364	4.2602300 +/- 0.0001	-1.09
	0.20	0.0237685679	0.2372860 +/- 0.0013	-1.30
	0.40	0.0630209469	0.6298750 +/- 0.0007	-0.76
	0.60	0.0197690310	0.1974930 +/- 0.0013	-0.77
	0.80	0.0499450801	0.4990640 +/- 0.0009	-0.86
	1.00	0.0028098955	0.0280769 +/- 0.0025	-0.31
	1.20	0.0130114830	0.1303950 +/- 0.0015	1.43
	1.40	0.0021885293	0.0218588 +/- 0.0037	-0.33
	1.60	0.1094651813	1.0941900 +/- 0.0004	-1.06
	2.00	0.0303790151	0.3037540 +/- 0.0007	-0.17
	2.20	0.0125587643	0.1256200 +/- 0.0011	0.23
	2.40	0.0342983395	0.3427940 +/- 0.0007	-0.79
	2.60	0.0050029697	0.0499229 +/- 0.0019	-1.13
	2.80	0.0120878717	0.1206850 +/- 0.0014	-1.15
	3.00	0.0028725969	0.0287638 +/- 0.0029	0.45
	3.20	0.0574927055	0.5753240 +/- 0.0007	0.99
	total	0.8647406141	8.6453300 +/- 0.0001	

Summary and Conclusions

Variance reduction for pulse-height tallies has been added to MCNP version 5.1.50. Applying variance reduction with pulse-height tallies is much more complicated than standard variance reduction techniques. It is critical to verify this new algorithm before release of MCNP 5.1.50. An analytic pulse-height tally problem has been previously defined but only partially analyzed. The analytic problem is continuous in space and discrete in energy and angle. Three ficticious isotopes were defined, each of which has a different photon-like nuclide. This work has completely analyzed this analytic problem and has provided high-precision numerical results for surface currents, surface fluxes, volume fluxes, energy deposited, and pulse-height spectrum. Calculated results from the latest available version of MCNP has been compared to the high-precision analytic solution for analog MCNP calculations and calculatings using many of MCNP's variance reduction techniques. The analytic results have been compared with MCNP calculations using both photon and coupled photon-electron transport. These calculated results matched the analytic values up to four or five significant figures with no value more than two standard deviations away from the analytic solution and follow the expected behaviour of a normal distribution. The verification process uncovered several subtle bugs in the first implementations of the variance reduction algorithm. Based upon the excellent agreement of all calculations with the analytic problem, the authors have greater confidence that the newly implemented feature to allow variance reduction with pulse-height tallies are correctly implemented in MCNP.

Acknowledgements

The authors would like to acknowledge Bryce J. Adams and Michael S. Reed who worked as summer students at LANL generating the analytic solutions and high-precision numerical results to this analytic problem. Additionally the authors would like to acknowledge the following people: Ted Shuttleworth for his creativity and useful discussions; Tom Booth and Roger Martz who helped make this document as correct and useful as possible; and Jeff Bull for his bulldog-like tenacity in identifying and solving coding issues with the addition of variance reduction for pulse-height tallies.

References

[1] X-5 Monte Carlo Team, "MCNP - A General N-Particle Transport Code, Version 5 - Volume I: Overview and Theory," Los Alamos National Laboratory report LA-UR-03-1987 (April 2003).

[2] Booth T.E., "Monte Carlo Variance Reduction Approaches for Non-Boltzmann Tallies," Los Alamos National Laboratory report LA-12433 (December 1992).

[3] Booth T.E., "Pulse Height Tally Variance Reduction in MCNP," Los Alamos National Laboratory report LA-13955 (August 2004).

[4] Booth, T.E. et al., "MCNP5.1.50 Release Notes," LA-UR-08-2300 (2008).

[5] T. Shuttleworth, "The Verification of Monte Carlo Codes in Middle Earth", Proceedings of the Eighth International Conference on Radiation Shielding, Arlington, Texas (1994).

[6] Personal communication (2002).

[7] Sood, A., Forster, R.A., Adams, B.J., and White, M.C.,"Verification of the Pulse-Height Tally in MCNP5," Nucl. Instr. and Meth. Phys. Res. B 213 (2004) 167-171.

[8] Sood, A., Reed M.S., and Forster, R.A.,"New Results for Pulse Hieght Tally Verification in MCNP5," Trans. Amer. Nucl. Soc. Vol. 89 456-457 (2003).